frontiers in Marine Science

ORIGINAL RESEARCH
published: 05 October 2021
doi: 10.3389/fmars.2021.520713

The Discovery and Preliminary Geological and Faunal Descriptions of Three New Steinahóll Vent Sites, Reykjanes Ridge, Iceland

James Taylor[1], Colin Devey[2], Morgane Le Saout[2], Sven Petersen[2], Tom Kwasnitschka[2], Inmaculada Frutos[3], Katrin Linse[4], Anne-Nina Lörz[5], Dominik Pałgan[6], Anne H. Tandberg[7], Jörundur Svavarsson[8], Daniel Thorhallsson[8], Adrianna Tomkowicz[6], Hrönn Egilsdóttir[9], Stefán Á. Ragnarsson[9], Jasmin Renz[1], Elena L. Markhaseva[10], Sabine Gollner[11], Eva Paulus[11], Jon Kongsrud[7], Jan Beermann[12,13], Kevin M. Kocot[14,15], Karin Meißner[1], Alexander Bartholomä[16], Leon Hoffman[16], Pauline Vannier[17,18], Viggó Þ. Marteinsson[17,18], Hans T. Rapp[19†], Guillermo Díaz-Agras[20], Ramiro Tato[20] and Saskia Brix[1]*

[1] Senckenberg am Meer, German Centre for Marine Biodiversity Research (DZMB) c/o Biocenter Grindel, Center of Natural History, Universität Hamburg, Hamburg, Germany, [2] GEOMAR Helmholtz Centre for Ocean Research Kiel, Kiel, Germany, [3] Department of Invertebrate Zoology and Hydrobiology, University of Lodz, Łódź, Poland, [4] British Antarctic Survey, Cambridge, United Kingdom, [5] Institute for Marine Ecosystems and Fisheries Science, Center for Earth System Research and Sustainability (CEN), University of Hamburg, Hamburg, Germany, [6] Institute of Oceanography, University of Gdańsk, Gdynia, Poland, [7] University of Bergen, University Museum of Bergen, Bergen, Norway, [8] Institute of Biology, University of Iceland, Reykjavík, Iceland, [9] Marine and Freshwater Research Institute, Hafnarfjörður, Iceland, [10] Zoological Institute, Russian Academy of Sciences, Saint Petersburg, Russia, [11] Department of Ocean Systems, Royal Netherlands Institute for Sea Research and Utrecht University, Texel, Netherlands, [12] Alfred Wegener Institute, Helmholtz Centre for Polar and Marine Research, Bremerhaven, Germany, [13] Helmholtz Institute for Functional Marine Biodiversity, Oldenburg, Germany, [14] Department of Biological Sciences, The University of Alabama, Tuscaloosa, AL, United States, [15] Alabama Museum of Natural History, The University of Alabama, Tuscaloosa, AL, United States, [16] Department of Marine Geology, Senckenberg am Meer, Wilhelmshaven, Germany, [17] Department of Research and Innovation, MATIS, Reykjavík, Iceland, [18] Faculty of Food Science and Nutrition, University of Iceland, Reykjavik, Iceland, [19] Department of Biological Sciences and K.G. Jebsen Centre for Deep-Sea Research, University of Bergen, Bergen, Norway, [20] Estación de Biología Marina de La Graña, Universidade de Santiago de Compostela, A Coruña, Spain*

OPEN ACCESS

Edited by:
Christopher Kim Pham, University of the Azores, Portugal

Reviewed by:
Mustafa Yucel, Middle East Technical University, Turkey
Daphne Cuvelier, Marine and Environmental Sciences Centre (MARE), Portugal

***Correspondence:**
James Taylor
james.taylor@senckenberg.de

†Died: 7th March 2020

Specialty section:
This article was submitted to Deep-Sea Environments and Ecology, a section of the journal Frontiers in Marine Science

Received: *16 December 2019*
Accepted: *31 August 2021*
Published: *05 October 2021*

Citation:
Taylor J, Devey C, Le Saout M, Petersen S, Kwasnitschka T, Frutos I, Linse K, Lörz A-N, Pałgan D, Tandberg AH, Svavarsson J, Thorhallsson D, Tomkowicz A, Egilsdóttir H, Ragnarsson SÁ, Renz J, Markhaseva EL, Gollner S, Paulus E, Kongsrud J, Beermann J, Kocot KM, Meißner K, Bartholomä A, Hoffman L, Vannier P, Marteinsson VP, Rapp HT, Díaz-Agras G, Tato R and Brix S (2021) The Discovery and Preliminary Geological and Faunal Descriptions of Three New Steinahóll Vent Sites, Reykjanes Ridge, Iceland. Front. Mar. Sci. 8:520713. doi: 10.3389/fmars.2021.520713

During RV *MS Merian* expedition MSM75, an international, multidisciplinary team explored the Reykjanes Ridge from June to August 2018. The first area of study, Steinahóll (150–350 m depth), was chosen based on previous seismic data indicating hydrothermal activity. The sampling strategy included ship- and AUV-mounted multibeam surveys, Remotely Operated Vehicle (ROV), Epibenthic Sledge (EBS), and van Veen grab (vV) deployments. Upon returning to Steinahóll during the final days of MSM75, hydrothermal vent sites were discovered using the ROV Phoca (Kiel, GEOMAR). Here we describe and name three new, distinct hydrothermal vent site vulnerable marine ecosystems (VMEs); Hafgufa, Stökkull, Lyngbakr. The hydrothermal vent sites consisted of multiple anhydrite chimneys with large quantities of bacterial mats visible. The largest of the three sites (Hafgufa) was mapped, and reconstructed in 3D. In total 23,310 individual biological specimens were sampled comprising 41 higher taxa. Unique fauna located in the hydrothermally venting areas included two putative new species of harpacticoid copepod (*Tisbe* sp. nov. and *Amphiascus* sp. nov.), as well as the sponge *Lycopodina cupressiformis* (Carter, 1874). Capitellidae Grube, 1862 and Dorvilleidae Chamberlin, 1919 families dominated hydrothermally influenced samples for polychaetes. Around the hydrothermally influenced sites we observed a

notable lack of megafauna, with only a few species being present. While we observed hydrothermal associations, the overall species composition is very similar to that seen at other shallow water vent sites in the north of Iceland, such as the Mohns Ridge vent fields, particularly with peracarid crustaceans. We therefore conclude the community overall reflects the usual "background" fauna of Iceland rather than consisting of "vent endemic" communities as is observed in deeper vent systems, with a few opportunistic species capable of utilizing this specialist environment.

Keywords: hydrothermal vent, VME, conservation, benthic fauna, infauna, bacteria, habitat, vent-associated

INTRODUCTION

Iceland is one of only two areas on Earth where a mid-ocean ridge has been elevated above the sea level, making it a remarkable laboratory for studying spreading-associated geological, biological, chemical, and physical processes (Sæmundsson, 1979). The island relief is a surface reflection of an underlying hotspot, which by interfacing with a mid-ocean ridge (i.e., Mid-Atlantic Ridge) makes it an ideal location to investigate the plume-ridge interaction and the effects it has on the evolution of Iceland and surrounding seafloor. The ∼26 Ma yearlong geological history of Iceland's development is directly correlated with the repeated eastward rift jumps that allowed the spreading center to remain fixed over the Icelandic hotspot (Sæmundsson, 1979; Foulger and Anderson, 2005; Martin et al., 2011).

The Geological Background

The Reykjanes Ridge (**Figure 1A**) is the longest oblique, hotspot-influenced section of the global mid-ocean ridge system (Talwani et al., 1971; Searle et al., 1998; Sandwell et al., 2014). This ∼950 km segment of the northern Mid-Atlantic Ridge is spreading at 1 cm y^{-1} half rate (Talwani et al., 1971; DeMets et al., 1990) and is located between Iceland (64°N) and the Bight Fracture Zone near 57°N. In general, the depth of the Reykjanes Ridge gradually shallows from south to north from ∼2500 m depth near Bight Fracture Zone (Keeton et al., 1997) to ∼300 m depth near 63°N (Pałgan et al., 2017). The ridge axis is divided into two morphological types: the area south of 59°N is defined by a prominent median valley (2.5 km deep and 15 km wide), while north of 59°N has a dome-shaped axial high; resembling mid-ocean ridges of higher spreading rate, e.g., East Pacific Rise (Talwani et al., 1971). The Reykjanes Ridge lacks first-order transform offsets (Keeton et al., 1997), but instead shows a short-wavelength segmentation composed of individual Axial Volcanic Ridges (AVRs) (Murton and Parson, 1993; Keeton et al., 1997; Searle et al., 1998). These ridges have a right-stepping echelon arrangement, are separated from one-another by 3–10 km of flatter seafloor, and usually overlap with each other in a spreading-parallel direction over a distance of one third of their length (Murton and Parson, 1993; Keeton et al., 1997; Searle et al., 1998; Höskuldsson et al., 2007; Pałgan et al., 2017). The surfaces of AVRs are characterized by either rough, untectonized, or clearly dissected tectonic deformation volcanic terrain. Volcanic features building AVRs include individual hummocks, hummocky ridges, fissure-, conical-, cratered- and flat-topped volcanoes up to several kilometers in diameter (Searle et al., 1998; Höskuldsson et al., 2007; Pałgan et al., 2017). It has been confirmed that the volcanic activity along the northern Reykjanes Ridge has been extensive throughout recorded times, with at least 14 documented eruptions between 63°10′N and Iceland (Thorarinsson, 1969; Jakobsson et al., 1978; Johnsson and Jakobsson, 1985; Höskuldsson et al., 2007). However, further south along the ridge, historic activity has not been documented and is unknown.

Hydrothermal activity has been poorly pinpointed along the Reykjanes Ridge. An extensive survey along the ridge was performed in 1990 (German et al., 1994). This led to the discovery of a hydrothermal plume near 63°06′N, which was called the namesake Steinahóll vent field. High concentrations of dissolved methane (18 nmol/1), hydrogen (30 nmol/1), silica (∼2 μmol/l), and total dissolvable manganese (∼60 nmol/l) characterize the vent plume. Moreover, the same plume was recorded by a high frequency (38 kHz) echosounder which mapped streams of bubbles rising from the seafloor. Due to technological limitations (lack of high-resolution bathymetric data) the data from German et al. (1994) could not precisely locate the source of the mapped plume. They indicated, however, that the field is located in the northern part of a prominent axial volcanic ridge (AVR). A cruise carried out in 2010 by the Marine and Freshwater Research Institute (Iceland) also observed areas of vent effluent indicated through the presence of bacterial mats (unpubl. obs.). More recent geological interpretations of that area by Pałgan et al. (2017), together with results from numerical modeling of fluid flow at mid-ocean ridges (Bani-Hassan et al., 2012), indicate that hydrothermal flow tends to focus toward topographic highs, suggesting that the Steinahóll Vent Field is located along a shallow (∼250 m depth) and 500 m long eruptive fissure situated between two east-facing faults. Hence, it has been suggested that the dikes intruding into the northern part of the AVR provide the heat necessary to drive hydrothermal flow while constant slip of the faults provides high crustal permeability (Pałgan et al., 2017).

Marine Vent Fields and Their Biology

The northern Reykjanes Ridge is a direct underwater continuation of the on-land fissures and volcanic systems of the southern Icelandic Reykjanes Peninsula (Jakobsson et al., 1978; Murton and Parson, 1993; Pedersen and Grosse, 2014; Pałgan et al., 2017), but relatively little is known about the volcanic and geothermal activity offshore (Hannington et al., 2001) and even less on the biological diversity of these active

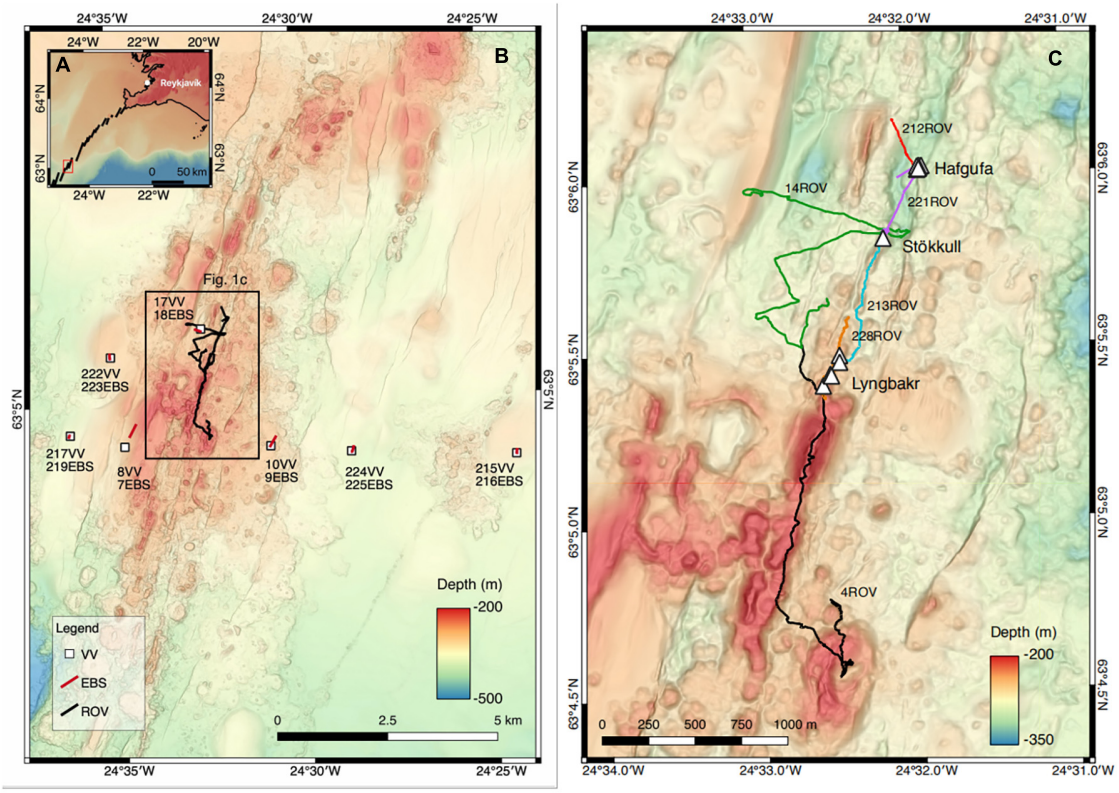

FIGURE 1 | (A) Regional map showing the northern section of the Reykjanes Ridge, indicated by a black line. The red box show the extent of the study area **(B)**. **(B)** Map of Steinahóll axial volcanic ridge at 5 m resolution with ROV tracks shown in black. The different sampling stations are located and named. Epibenthic sled (EBS) track are shown by a red line, ROV dive track by a black line, and Van Veen grab (vV) position is indicated by white squares. The black box shows the extent of **(C)**. **(C)** Map of the Steinahóll vent sites. Hydrothermal vents (white triangles) are grouped in three hydrothermal field named Hafgufa, Stökull, and Lyngbakr. Venting is indicated by white triangles. ROV dives are individualized by different color lines.

sites (Fricke et al., 1989; Eythorsdottir et al., 2016). Over the last decades, information has been published on the biodiversity of the known hydrothermal vent fields on the Mid-Atlantic Ridge (MAR) and the Arctic Mid Ocean Ridge (AMOR). To date in the North Atlantic, the biology of 12 vent fields along the MAR has been described for the area between 12° and 45°N, at depths ranging from 850 to 4200 m (Desbruyères et al., 2000; 2006; Wheeler et al., 2013). At the same time, biology has been studied on only few shallow water vent fields (≤500 m deep), e.g., Kolbeinsey at AMOR (located at depth of ∼100 m, Fricke et al., 1989). Moreover, only bacterial studies have been carried out along the AMOR (Wheeler et al., 2013). The macrofauna of the deep MAR vent fields is characterized by the presence of vent-endemic and chemosynthetic taxa, dominated by such as the alvinocarid shrimps *Mirocaris* Vereshchaka, 1997 and *Rimicaris* Williams and Rona, 1986, the bivalve *Bathymodiolus* Kenk and B.R. Wilson, 1985 or the gastropod *Peltospira* McLean, 1989 (e.g., Desbruyères et al., 2000, 2006; Tarasov et al., 2005; Wheeler et al., 2013).

Van Dover et al. (2018) describe hydrothermal vent ecosystems as "natural wonders of the ocean" that help us to understand the intersection of life and Earth processes, and are acting as storehouses of endemic marine genetic diversity. Under the United Nations General Assembly (UNGA) resolution 61/105, management of fisheries in areas beyond national jurisdiction requires identification of vulnerable marine ecosystems (VMEs). Criteria to designate a VME include uniqueness, functional significance, fragility, structural complexity, and certain life history traits. Hydrothermal vent fields can be viewed as small islands within the different habitats of the ocean floor, being colonized by endemic and mostly rare species (Van Dover et al., 2018). They show such a high natural variability that it is difficult to designate a "representative" ecosystem in the northern MAR according to the work of Desbruyères et al. (2000), wherein species composition and abundances at eight known active vents along the MAR in the North Atlantic are compared. Their results exemplify the ecological rarity and vulnerable status of active hydrothermal vents. Statutes for full protection of ecosystems at active hydrothermal vents have been enacted by several coastal States (e.g., Canada, Mexico, New Caledonia, Portugal, United States) through establishment and management of area-based protection (LeBris et al., 2016). Furthermore, the Oslo and Paris Commission for the Convention for the Protection of the Marine Environment of the North-East Atlantic (OSPAR) recommends protection and conservation of hydrothermal vent

fields as "priority habitats" (OSPAR, 2008, 2014) in the OSPAR maritime area (NE Atlantic). Similar reasoning, with the aid of advice from organizations such as The International Council for the Exploration of the Sea (ICES), has lead the North-East Atlantic Fisheries Commission (NEAFC) to restrict and close certain areas of the NE Atlantic for certain fishing practices. Thus, active vents are recognized as vulnerable through multiple international instruments that call for their protection.

Tarasov et al. (2005) state that hydrothermal vent communities split into a "shallow-water" (<200 m) and a "deep-sea" (>200 m) group, with the former having none or few vent-obligate taxa, while the latter is characterized by chemosynthetic vent-endemic taxa. They postulate that the proportion of organic matter derived from photosynthesis and chemosynthesis might play a crucial role in the evolutionary history of the faunal communities. Over the recent decades, the benthic fauna around Iceland has been subject to comprehensive biodiversity surveys under the umbrellas of the international projects BIOICE (Benthic Invertebrates of Icelandic waters; 1992–2004) and IceAGE (Icelandic marine Animals: Genetics and Ecology; 2011—ongoing), encompassing 23 research cruises and samples from more than 1700 locations (Brix et al., 2014a,b; Meißner et al., 2014). While the benthic megafauna of the Reykjanes Ridge from the shelf to the lower bathyal zones has been studied thoroughly in the past (Copley et al., 1996), during IceAGE samples were taken to compare stations on the East and West side of the Reykjanes Ridge (Brix et al., 2018a,b). However, no focused biological sampling has been done in close proximity to hydrothermally active sites of Steinahóll before this study. Previous cruises conducted in the area by the Icelandic Marine and Freshwater Research Institute (MFRI) (2004 and 2010) and Ifremer/MFRI (2012), with the goal of researching coral reefs and fishing impacts, have yielded large quantities of video/image material, of which contains indications of hydrothermal activity (unpubl. obs.), aiding in location selection for the dives accomplished during MSM75 cruise.

Hunting the Steinahóll Vent Sites, Discovery, and Preliminary Descriptions of the Geological and Biological Composition

Steinahóll was detected in 1990 during a response cruise following a seismic event south of Iceland (Palmer et al., 1995). Water column studies, echosounding and towed video indicated the presence of a hydrothermal plume that was later confirmed and more precisely located in 1993 near 63°06′N, 24°32′W (German et al., 1994). Based on the coordinates given in German et al. (1994) and previous cruise reports by French and Icelandic projects, our aim was first to detect and bathymetrically map the exact location of the Steinhóll vent field and the surrounding area. More importantly, the mapping is accompanied by the first biological description of faunal communities proximal and distal to the venting sites. We hypothesized from our knowledge of two shallow-water venting sites North of Iceland, that the Steinahóll fauna resembles the adjacent fauna as already described from the Mohns (Schander et al., 2010) and Kolbeinsey Ridges (Fricke et al., 1989). However, the fauna at Steinahóll should vary from those found at the vent sites in the North. This is based on our knowledge about the different biogeographic regions and faunal composition in the Arctic water mass influenced north and the Atlantic water mass influenced south of Iceland (Brix and Svavarsson, 2010; Dauvin et al., 2012; Jochumsen et al., 2016; Brix et al., 2018a,b).

During the final days of the expedition MSM75 we discovered what could be interpreted as the previously detected vent fields, after a previous search in the area which had proven unfruitful. Upon locating the vent fields, our geological aim was to map and document the discovery. The aim of the biological part of this study was to give an introductory description of potential vent-influenced fauna compared to non-vent-influenced fauna at the Steinahóll area of the Reykjanes Ridge. We also compare this to other shallow reduced habitats examined in the North Atlantic. This is part of ongoing assessment in the area with further expeditions planned.

MATERIALS AND METHODS

Deployment of Sampling Gear

During the research cruise MSM75 onboard the R/V *Maria S. Merian* between June and August 2018, we mapped the Steinahóll area using the ship's hull-mounted Kongsberg EM712 75 kHz echo-sounder at a speed of 5 knots. The shallow depth along the ridge (less than 500 m) allowed a 5 m resolution to be achieved (**Figure 1B**). In addition to the bathymetric maps, Steinahóll was also surveyed by the Autonomous Underwater Vehicle (AUV) Abyss from GEOMAR equipped with an Edgetech sidescan sonar 2200-S 120/410 kHz and with turbidity, CTD, and redox potential sensors. The combined data were used to target potential hydrothermally active sites and to plan further dives with the Remotely Operated Vehicle (ROV) Phoca from GEOMAR.

During ROV deployments, samples were collected using the operational arm, net, and scoop. Overall 19 samples yielding biological results were taken (10 via arm, 8 via net, and 1 via scoop). A complete station list of the IceAGE project is available via OBIS (Brix and Devey, 2019). Further biological samples (**Tables 1**, **2**) were taken with an epibenthic sled (EBS; Brenke, 2005) and van Veen grab (vV; van Veen, 1933). Locations for EBS and vV sampling were chosen with a minimum distance of 1 km from discovered vent activity, and using bathymetric maps from the AUV and backscatter data to ensure the presence of "soft bottom" areas. Prior to each EBS deployment, a vV was deployed adjacent to the planned EBS track to recover sediment samples and to verify the composition of the bottom substrate, ensuring to the best of our abilities that venting areas were protected. EBS and vV samples were taken at different distances from the Steinahóll vent site. All EBS trawls, after the third deployment (station 24EBS), were equipped with a Sonardyne system ultra-short baseline (USBL) pinger (ranger 2712) to provide maximum precision in EBS positioning. The trawl distance for EBS deployments was 300 m. In total, we deployed six vV grabs

TABLE 1 | Station list of biological sampling locations; *: hydrothermally influenced sample.

Station	Dive/Deployment No.	Gear (Sampling equipment)	Cast	Date	Start°N and°W - End°N and° W	Depth (m)
MSM75-4	**ROV 4**	**ROV**		01.07.18	63°05.496′/24°32.569′ -63°04.744′/24°32.485′	200–245
		(Arm)	*1*		*63°04.404′/24°32.634′*	*233*
		(Arm)	*2**		*63°05.376′/24°32.587′*	*225*
		(Net)	*4*		*63°04.707′/24°32.771′*	*242*
		(Arm)	*5*		*63°04.645′/24°32.632′*	*205*
		(Net)	*6**		*63°04.597′/24°32.521′*	*242*
MSM75-13	**ROV 13**	**ROV**	*Video only*	03.07.18	63°05.521′/24°32.525′–63°05.523′/24°32.775′	230–261
MSM75-14	**ROV 14**	**ROV**		03.07.18	63°05.588ß/24°32.552′ –63°06.039′/24°33.177′	253–300
		(Arm)	*3*		*63°05.901′/24°32.833′*	*295*
MSM75-212	**ROV 212**	**ROV**		03.08.18	63°06.100′/24°32.007′–63°05.965′/24°31.905′	289–315
		(Arm)	*1**		*63°06.028′/24°31.918′*	*310*
		(Net)	*2**		*63°06.024′/24°31.918′*	*310*
		(Net)	*3**		*63°06.026′/24°31.916′*	*311*
		(Arm)	*4**		*63°06.012′/24°31.918′*	*308*
		(Arm)	*5**		*63°06.014′/24°32.129′*	*306*
MSM75-213	**ROV 213**	**ROV**		03.08.18	63°05.829′/24°32.139′–63°05.443′/24°32.517′	157–260
		(Net)	*1**		*63°05.830′/24°32.147′*	*259*
		(Net)	*3*		*63°05.482′/24°32.472′*	*235*
MSM75-228	**ROV 228**	**ROV**		05.08.18	63°05.623′/24°32.449′–63°05.407′/24°32.544′	250–274
		(Net)	*1**		*63°05.484′/24°32.461′*	*236*
		(Scoop)	*2*		*63°05.488′/24°32.477′*	*234*
		(Arm)	*3*		*63°05.488′/24°32.478′*	*234*
		(Arm)	*5**		*63°05.430′/24°32.522′*	*235*
		(Arm)	*6*		*63°05.430′/24°32.516′*	*239*
		(Net)	*7*		*63°05.361′/24°32.564′*	*211*
MSM75-7	**EBS 7**	**EBS**		02.07.18	63°04.687′/24°34.581′ –63°04.619′/24°34.665′	250–277
MSM75-9	**EBS 9**	**EBS**		02.07.18	63°04.469′/24°30.849′ –63°04.433′/24°30.897′	293–286
MSM75-18	**EBS 18**	**EBS**		04.07.18	63°05.889′/24°32.741′ –63°05.898′/24°32.794′	294–293
MSM75-216	**EBS 216**	**EBS**		03.08.18	63°04.348′/24°24.238′ –63°04.348′/24°24.239′	314–315
MSM75-219	**EBS 219**	**EBS**		03.08.18	63°04.563′/24°36.326′ –63°04.564′/24°36.324′	356–355
MSM75-223	**EBS 223**	**EBS**		04.08.18	63°05.708′/24°35.154′ -63°05.708′/24°35.155′	281-281
MSM75-225	**EBS 225**	**EBS**		04.08.18	63°04.470′/24°28.623′ -63°04.470′/24°28.623′	360-359
MSM75-8	**vV 8**	**vV**		02.06.18	63°04.520′/24°34.784′	286
MSM75-10-1	**vV 10-1**	**vV**		02.07.18	63°04.443′/24°30.876′	286
MSM75-10-2	**vV 10-2**	**vV**		02.07.18	63°04.441′/24°30.875′	286
MSM75-17	**vV 17**	**vV**		04.07.18	63°05.903′/24°32.648′	302
MSM75-215	**vV 215**	**vV**		03.08.18	63°04.239′/24°24.260′	323
MSM75-217	**vV 217**	**vV**		03.08.18	63°04.652′/24°36.270′	360
MSM75-222	**vV 222**	**vV**		04.08.18	63°05.582′/24°35.155′	291
MSM75-224	**vV 224**	**vV**		04.08.18	63°04.343′/24°28.707′	363

and seven EBS. Overall, there were six deployments (dives) of the ROV Phoca. ROV biological sampling took place at 19 discrete locations, sampling hydrothermally active localities with bacterial mats and inactive localities for comparison. Specifically, the Steinahóll vent field explored during the ROV dives was sampled in regard to bacterial mats and vent-associated macrofauna using nets with a mesh size of 1 mm, and scoops of sediment were taken and transferred to closable bioboxes.

Samples were washed in chilled, filtered seawater directly on board, with EBS and vV samples being sieved through four size classifications (1 cm, 1 mm, 500 μm, and 300 μm). All samples were live-sorted for large specimens over the period of 1 h after sampling and treated "on ice" (Riehl et al., 2014). After the live sorting, all specimens were immediately fixed either in –20°C precooled 96% undenatured ethanol, RNAlater, 4% buffered formaldehyde solution, or frozen at –80°C. RNAlater and frozen samples were photographed and stored along with a representative sample specimen fixed in 96% undenatured ethanol. Sorting of the Steinahóll samples was finalized in the laboratory of the DZMB Hamburg, Germany using Leica MZ 12.5 binocular microscopes.

TABLE 2 | Faunal composition showing total individuals of each taxa sampled at the Steinahóll vent fields.

	Gear	ROV					EBS							vV						
Taxa	**Station**	**4**	**14**	**212**	**213**	**228**	**7**	**9**	**18**	**216**	**219**	**223**	**225**	**8**	**17**	**215**	**217**	**222**	**224**	**Total**
Porifera																				
Porifera		19	2	2	–	26	47	1	4	2	–	2	80	–	11	–	5	18	20	**239**
Cnidaria																				
Anthozoa		–	–	–	–	1	5	1	–	–	–	–	2	–	–	–	1	–	1	**11**
Hydrozoa		10	1	–	14	–	33	–	–	–	–	1	–	–	–	10	1	36	–	**106**
Ctenophora																				
Ctenophora		–	–	–	–	–	–	–	–	–	1	–	–	–	–	–	–	–	–	**1**
Annelida																				
Polychaeta		280	2	255	146	755	1766	20	1	102	4	7	399	2	59	81	132	126	194	**4331**
Oligochaeta		13	–	19	4	7	53	–	–	–	–	–	–	–	5	–	1	1	–	**103**
Sipuncula																				
Sipuncula		2	–	2	–	3	6	–	–	2	–	–	5	–	1	4	3	4	3	**35**
Platyhelminthes																				
Platyhelminthes		–	–	–	–	–	4	–	–	–	–	–	–	–	–	–	–	–	–	**4**
Cephalorhyncha																				
Priapulida		–	–	–	1	1	–	–	–	–	–	–	–	–	1	–	–	–	–	**3**
Mollusca																				
Aplacophora		–	–	4	–	–	49	–	–	4	–	–	7	–	–	2	4	2	2	**74**
Bivalvia		14	–	–	–	2	141	2	1	139	3	–	109	–	9	46	16	12	34	**528**
Cephalopoda		–	–	–	–	–	–	–	–	–	–	–	1	–	–	–	–	–	–	**1**
Gastropoda		18	–	3	–	7	271	4	–	16	2	–	–	1	3	1	1	1	–	**328**
Polyplacophora		–	–	–	–	1	17	–	–	–	–	–	–	–	2	–	–	–	–	**20**
Scaphopoda		–	–	–	–	–	98	–	–	–	30	–	19	–	1	12	1	19	6	**186**
Arthropoda																				
Pycnogonida		1	–	–	–	–	40	2	–	4	1	–	3	–	–	1	–	–	–	**52**
Acarina		2	–	4	–	6	–	–	–	–	–	–	–	–	–	–	–	–	–	**12**
Crustacea																				
Ostracoda		50	–	–	1	13	372	9	–	16	1	1	43	–	12	1	6	6	74	**605**
Copepoda Calanoida		43	–	8	8	14	795	501	1335	920	79	524	2079	–	14	8	35	26	201	**6590**
Copepoda Harpacticoida		33	–	173	14	1109	54	–	–	–	–	–	1	–	–	–	1	1	1	**1387**
Cirripedia		–	–	–	1	–	1	–	–	–	–	–	–	–	–	–	–	–	–	**2**
Leptostaca		–	–	–	–	2	5	–	–	–	–	–	–	–	–	–	–	–	–	**7**
Amphipoda		258	–	60	66	356	1299	8	2	29	2	3	101	2	33	15	23	16	5	**2278**

(Continued)

TABLE 2 | (Continued)

	Gear	ROV					EBS							vV						
Taxa	**Station**	**4**	**14**	**212**	**213**	**228**	**7**	**9**	**18**	**216**	**219**	**223**	**225**	**8**	**17**	**215**	**217**	**222**	**224**	**Total**
Cumacea		–	–	1	–	1	474	1	–	32	2	1	55	–	–	–	–	–	2	**569**
Isopoda		52	–	24	1	35	463	13	1	6	1	2	87	–	21	5	6	9	5	**731**
Mysida		–	–	–	1	2	51	1	1	10	1	–	69	–	–	–	–	–	–	**136**
Tanaidacea		2	–	5	–	2	54	1	–	–	–	3	2	–	3	–	5	7	4	**88**
Euphausiacea		–	–	1	1	–	–	–	5	2	–	–	–	–	–	–	–	1	–	**10**
Decapoda		–	–	–	–	–	5	1	–	–	–	–	–	–	–	–	–	–	–	**6**
Echinodermata																				
Asteroidea		–	–	–	–	–	7	–	–	–	–	–	–	–	–	–	–	–	–	**7**
Ophiuroidea		21	1	1	4	7	2323	7	2	59	1	2	62	–	–	–	–	–	–	**2490**
Crinoidea		–	–	–	–	–	5	–	–	–	–	–	4	–	–	–	–	–	–	**9**
Echinoidea		2	–	–	–	–	–	–	–	–	–	–	–	1	1	–	–	–	–	**4**
Holothuroidea		1	–	–	–	–	91	–	–	11	1	–	43	–	2	3	2	6	20	**180**
Brachiopoda																				
Brachiopoda		20	–	–	–	–	12	–	–	1	–	–	–	1	1	–	1	5	–	**41**
Bryozoa																				
Bryozoa		11	–	–	6	10	41	–	7	4	1	5	28	–	–	3	2	24	5	**147**
Chaetognatha																				
Chaetognatha		–	–	–	–	4	17	1	–	–	–	3	9	–	–	–	–	–	–	**34**
Nematoda																				
Nematoda		687	–	65	1	176	472	7	1	3	–	1	19	–	20	9	194	111	23	**1789**
Nemertea																				
Nemertea		29	–	14	24	11	22	–	–	2	–	–	–	1	–	–	1	1	6	**111**
Hemichordata																				
Enteropneusta		–	–	–	–	–	32	–	–	–	–	–	–	–	1	–	–	–	–	**33**
Chordata																				
Tunicata		–	–	–	–	–	17	–	–	–	–	3	–	–	1	–	–	–	1	**22**
	Total	1568	6	641	293	2551	9142	580	1360	1364	130	558	3227	8	201	201	441	432	607	**23310**

For the photogrammetric surveys a CANON Eos 6D SLR of 20 MP resolution with a 15 mm fisheye lens (CANON 8–15 mm f4.5 zoom) was employed as part of the DeepSurveyCam package described in Kwasnitschka et al. (2016). This system was developed for the GEOMAR AUV Abyss and uses a high power LED strobe. Of the three strobe arrays normally employed only two were carried on either manipulator of the ROV. The mounting of the strobe arrays onto the manipulator arms meant it was possible to precisely adapt the illumination pattern to the requirements of the terrain. The camera was mounted on the starboard front porch on a hydraulic tilt unit, oriented in landscape mode relative to the direction of travel. Visibility varied between sites due to varying particulate matter in the water column, so an optimum altitude of four meters was aimed for. Useful results were gathered at up to 6 m altitude while the continuity of the reconstruction could still be maintained at 8 m altitude. At an across track field of view of 160°, we obtained a track width of approximately 15 m, limited by scattering and absorption. Minimum altitude was around 2 m dictated by the amount of overlap between each image.

As an important note, we point out that, as typical for an exploratory scientific cruise, samples were not taken quantitatively and without direct replicates for each station.

Data Analysis

The ship-based bathymetry was post-processed on board using QPS Qimera software and its 3D Swath Editor to flag false data. The processed data was then exported and integrated in the open source software QGIS and used as based map for preliminary geological interpretations and the plan of ROV dive tracks and sampling stations.

Chimney samples and crusts were described macroscopically on board for their major mineralogical components. Further investigation of trace minerals and geochemical composition are pending. The van Veen sediment samples have been dialyzed to remove the salt. The separation of the sand fraction (>63 μm) and the mud fraction (<63 μm) has been realized by wet sieving with a mesh size of 63 pm. The grain-size analyses of the dispersed sediments were performed by a Sedigraph5100 (Micromeritics^{TM}) particle analyzer (see e.g., Bianchi et al., 1999). The system determines the size distribution of particles dispersed in a liquid assuming Stokes' Law of settling. It measures the attenuation of a finely collimated X-ray beam as a function of time and height in a settling suspension. By means of the standard Micro-meritics software (version 3·07) for the Sedigraph the changes of attenuation over time were transformed into grain size fraction ranging from coarse of silt to clay.

Photogrammetric 3D reconstructions were done using the Agisoft Photoscan Pro software as detailed in Kwasnitschka et al. (2016). Processing involved the correlation and cross-referencing of USBL and DVL navigation records, which then served as a first order pose estimation to initialize the photogrammetric reconstruction and, together with multibeam maps, form the basis for georeferencing of the reconstructions. Camera orientation was logged inside the camera housing and was fused with other navigation information.

Upon review of the ROV and EBS samples it was evident that Porifera were underrepresented compared with what was observed during the ROV dives. This is predominantly due to the Porifera inhabiting hard bottom substrata, including large pillow larva. As we did not use the EBS in these areas for protection and the ROV being used for mainly exploratory purposes, it was decided to use the HD front-view video for qualitative (presence/absence) registration of Porifera, as well as noting their proximity to venting areas.

The preliminary results of the microbial diversity were obtained by 16S rRNA gen sequencing, Samples were collected and conserved for molecular analysis and for cultivation of microbes.

RESULTS

Hydrothermal Vent Field Discovery and Naming the Single Venting Spots

In order to help identify areas of hydrothermal activity, the ship-based multibeam echosounding system was used in the water-column mode in order to detect bubble streams. The newly discovered vent fields were given names of traditional maritime mythological folk creatures (Illhveli; "evil-whales") thought to reside in the treacherous waters surrounding Iceland so to represent and reflect the local culture and traditions.

We named the largest vent field (**Figure 1**) "Hafgufa," known in multiple folklores as the Kraken. The first known record of Hafgufa (haf = ocean; gufa = steam) is in the 12th century Norwegian saga Konungsskuggsjá (Kings mirror). In Örvar-Odds saga, an Icelandic saga from the 13th century, the creature is described as an enormous and evil beast, able to devour whole ships along with its men. At low tide, her nose would rise out of the water to be mistaken for two massive rocks rising from the sea.

The Southernmost vent field is named "Lyngbakr" (Lyng = heather; bakr = back) from Örvar-Odds saga. Lyngbakr is an enormous whale-like beast with a back that resembles a heather strewn island. Unlike Hafgufa is thought to be benign, but if unsuspecting seafarers take land on its back, often mistaking the creature's eyes as pools of freshwater, they may drown if Lyngbakr decides to dive.

The Illhveli "Stökkull" (stökk = jump) was used to name the middle vent field and is described in Íslenzkar þjóðsögur og aevintýri, 1862, edited by Jón Árnason. Stökkull would jump out of the sea and onto ships, leaving them in danger of sinking to the bottom of the sea. To prevent this, Saint Brendan requested divine intervention, receiving it in large flaps that covered the creature's eyes, rendering it blind. However, this did not prevent the creature from maintaining its destructive strategy and nature, remaining a threat to those ships unfortunate to encounter one.

Hafgufa

Indications for gas venting were observed 1.4 km north of the shallowest point of the Steinahóll area. These indications were later confirmed to originate from a dense area of venting with

dimensions of 60 m in N/S direction and a width of 35 m (Hafgufa; **Figure 1C**). Hafgufa is located at a water depth of ca. 300 m, close to the first fault on the eastern ridge flank in this area. The vent site was associated with pillow lava and located in the hanging-wall of the fault, with its location appearing to follow a ridge-parallel fault trace in the sub-sea floor. Hydrothermal activity was shown by small anhydrite chimneys, commonly < 1 m in height, and abundant bacterial mats. Some of the chimneys sat on small mounds (only a few meters in diameter; **Figures 2A,B**) consisting of sand-sized talus material, as well as siliceous and barite-bearing slabs (**Figure 2C**). The largest of the mounds, also hosting the largest chimney ("Central Chimney" 2.5 m in height) had a diameter of approximately 7 m. The chimneys were located at the periphery of small depressions, the largest of these being 15 m in diameter. Additional small depressions were located just south of the largest chimney and were aligned parallel to the fault scarp in the east. The elevated rim around the depressions consisted of clay-rich hydrothermal precipitates and talus material, including crusts. This indicates that hydrothermal activity has been present in the area for some time. The formation of the depressions is likely the result of the collapse of anhydrite-bearing material during waning stages of hydrothermal activity, as anhydrite has a retrograde solubility and dissolves in cold seawater. This process has been

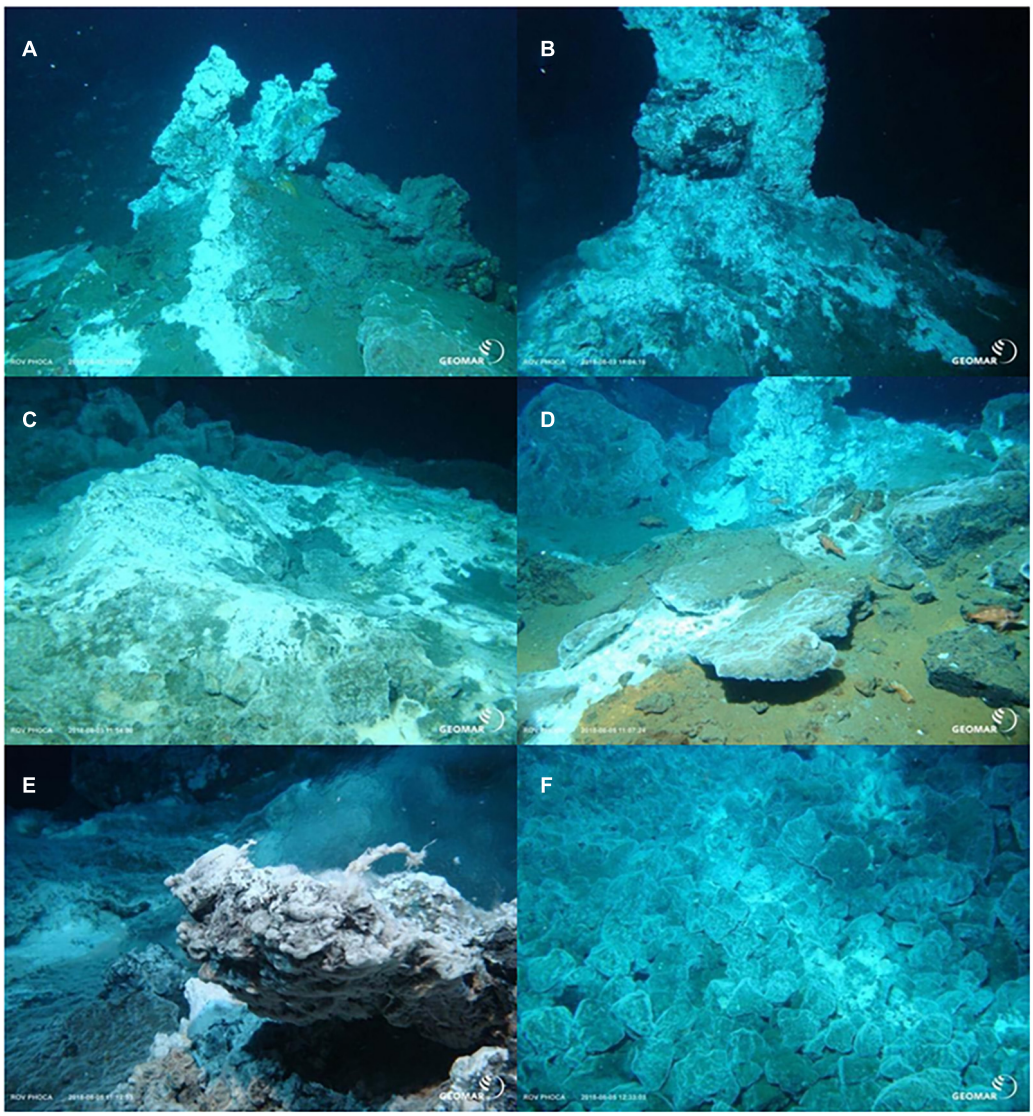

FIGURE 2 | (A) Small anhydrite chimney with associated bacterial mats located on top of a small mound at Hafgufa (212ROV-T11:33). **(B)** Base of largest chimney (2.5 m height) observed in the Steinahóll area. The chimney at Hafgufa is largely composed of anhydrite with minor pyrite/marcasite (212ROV-T11:04). **(C)** Small circular depression at Hafgufa with raised clay- rich rim covered in microbial mats. The elevated nature of the rim indicates a hydrothermal formation while anhydrite dissolution might be responsible for the formation of the depression (212ROV-T11:54). **(D)** Vent site at Lyngbakr with large anhydrite blocks, bacterial mats, and siliceous crusts in the foreground. Iron-staining is visible in the sediments (228ROV- T11:07). **(E)** Diffuse venting of clear fluids from a small chimney at Lyngbakr. All rock surfaces are covered by bacterial mats (228ROV-T11:12). **(F)** Bacterial mats coating basaltic talus indicating more widespread diffuse venting (228ROV-T12:33).

invoked for the formation of breccias at the active TAG mound (Humphris et al., 1995) and for similar depressions in the serpentinite-hosted Logatchev hydrothermal field (Petersen et al., 2009). Fluid flow was subdued and consisted of transparent fluids containing gas bubbles. Filamentous bacterial mats were present in areas of diffuse fluid venting, as well as covering larger areas of the seafloor. Bacterial mats were also widespread in talus piles indicating diffuse venting from below through the highly permeable pillow talus material. Together with anhydrite from chimneys (**Figure 3A**) a few massive to semi-massive pyrite-marcasite-bearing sulfides (**Figure 3B**) have been collected from underneath siliceous barite-rich slabs (**Figures 3C,D**) while Fe-oxyhydroxides were rare. Photometric surveys during ROV 221 allowed the mapping and 3D reconstruction of Hafgufa (**Supplementary Figure 1**).

Stökkull

Subsequent ROV dives located small patches of venting along the central volcanic chain itself. These sites, each only a few meters in diameter, were not connected to ridge-parallel faults and the heat distribution was along pillow margins, talus pieces, and cracks in the youngest volcanic rocks. Gas bubbles were observed at all chimneys. The second vent site was located 400 m south of Hafgufa and consisted of isolated patches of hydrothermal venting with bacterial mats, hydrothermal crusts, and small (<1 m in height) anhydrite chimneys (259 m water depth; **Figure 1C**).

Lyngbakr

Additional, more isolated, anhydrite chimneys and associated hydrothermal crusts were found in a water depth of around 235 m, closer to the local axial high. The sites are distributed over a strike length of 300 m with all chimneys occurring in a water depth of around 235 m. The northernmost site of Lyngbakr is located 700 m south of Stökkull (Lyngbakr; **Figure 1C**). Again, anhydrite-chimneys and siliceous crusts dominated the hydrothermal precipitates. As with the Stökkull site, individual vent sites at Lyngbakr are only a few meters in diameter. These vent sites were characterized by diffuse fluid venting and bacterial mats on the surrounding talus material (**Figures 2D–F**).

Biological Description of Steinahóll

Higher Taxon/Family Level

In total 23,310 individual specimens were collected and identified (to varying taxonomic levels, dependant on group) over the span of six ROV (5,059 ind.), seven EBS (16,361 ind.), and six vV (1,890

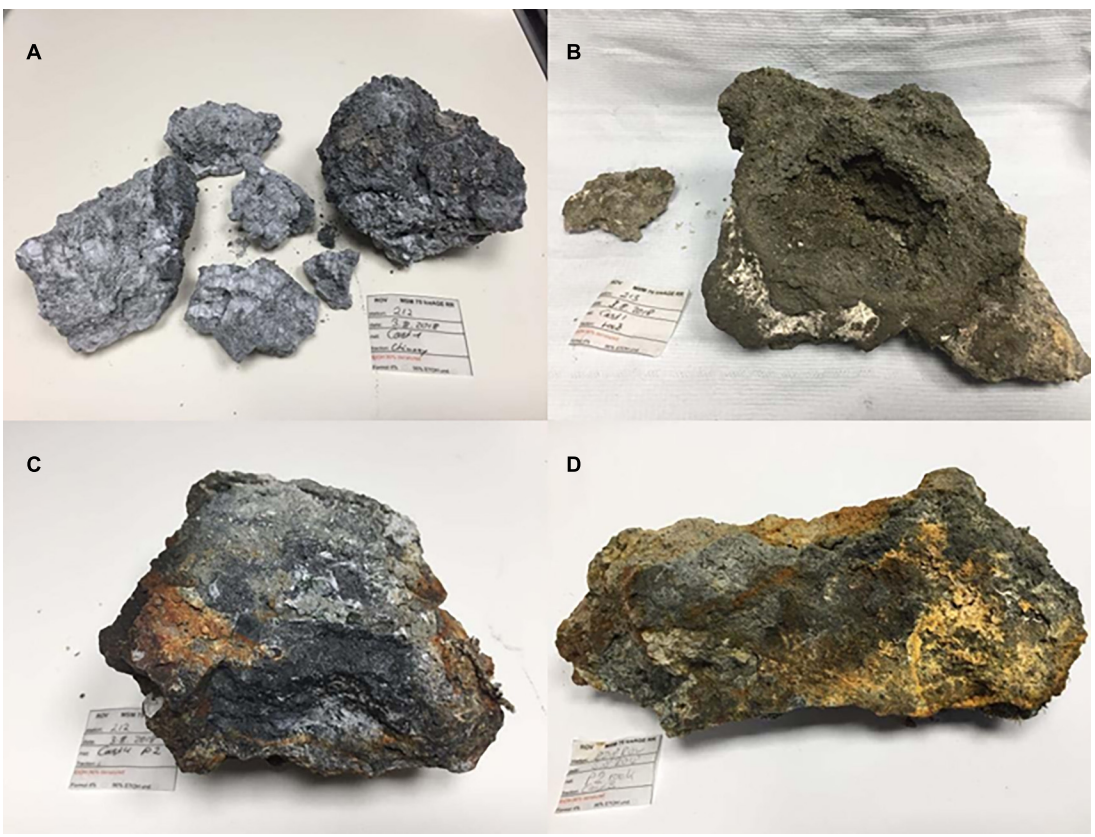

FIGURE 3 | (A) Massive coarse-grained anhydrite from chimney in the Steinahóll field. **(B)** Massive pyrite-marcasite collected from underneath siliceous slabs indicating reduced conditions in the immediate subseafloor. The sample is upside down, the overlying, white siliceous and barite-rich cap can be seen. **(C)** Brecciated hydrothermal crusts colored dark from fine-grained sulfides. **(D)** Large siliceous slab showing Fe-oxyhydroxide staining and remnants of bacterial mats. Sampling card is 4 cm across.

ind.) deployments. These specimens were assigned to a wide range of phyla, spanning 41 taxonomic groupings used further for comparison of faunal community in this study (**Table 2**), with taxonomic composition of each sampling effort visible in **Figure 4**. Full tables of sampled Polychaeta, Amphipoda, Isopoda, Mollusca, and harpacticoid Copepoda to family level are provided in the **Supplementary Tables 1–5**, respectively.

Observations made during ROV deployment also showed large numbers of fish in the area, as well as a number of cold-water corals, which were unable to be physically sampled during our efforts. However, as the area of study was located within Icelandic territorial waters, we observed evidence of fishing pressure through discarded long-line and gill-net equipment (**Figure 5**).

Vent-Associated Fauna

Steinahóll was categorized biologically by two distinct habitats, rocky areas with relatively low densities of visible megafauna (except large quantities of various fish species) and hydrothermally active sites, containing wide coverages of bacterial mats. The megafaunal composition comprised crustaceans, sponges, echinoderms, corals, reef building polychaetes, molluscs, fish, and ascidians.

Video-based observations

Porifera. The sponge fauna on this section on the Reykjanes Ridge appears to be very rich with several types of sponge communities existing side by side. By applying a very conservative approach, 39 taxa (ranging from species level to class) were identified from the ROV footage (**Supplementary Table 6**). ROV 14 contained the highest number of taxa as well as most dense sponge communities (31 out of the total of 39), while in the ROV dives 212, 213, 221, and 228, only 2–6 sponge taxa were observed. The high sponge richness and abundance were confined to areas outside of the active venting, and the transition zones between soft sediments and various cold-water corals. Only one species, *Lycopodina cupressiformis* (Carter, 1874), was found within the area of active venting, while *Asbestopluma (Asbestopluma) furcata* (Lundbeck, 1905), Cladorhiza Sars, 1872 sp., unidentified Axinellidae Carter, 1875, and unidentified encrusting sponges were found in areas with more diffuse venting and bacterial mats or filaments.

Hard and soft substrates in the close surroundings of the vents hosted sponge faunas of both boreal and more temperate affinities. The most abundant boreal species included *Geodia atlantica* (Stephens, 1915), *G. barretti* Bowerbank, 1858, *G. macandrewii* Bowerbank 1858, *G. phlegraei* (Sollas, 1880), *Stelletta* Schmidt, 1862 sp., *Mycale (Mycale) lingua* (Bowerbank, 1866), *Petrosia crassa* (Carter, 1876) and *Asconema* cf. *foliatum* (Fristedt, 1887). The more temperate fauna was highly dominated by glass sponges, with *Euplectella suberea* Thomson, 1876, *Hyalonema (Cyliconema) thomsonis* Marshall, 1875, *Pheronema carpenteri* (Thomson, 1869), *Aphrocallistes* cf. *beatrix* Gray, 1858, Euretidae Zittel, 1877 indet., and *Asconema* Kent, 1870 spp. being the most abundant species. In addition, *Geodia megastrella*

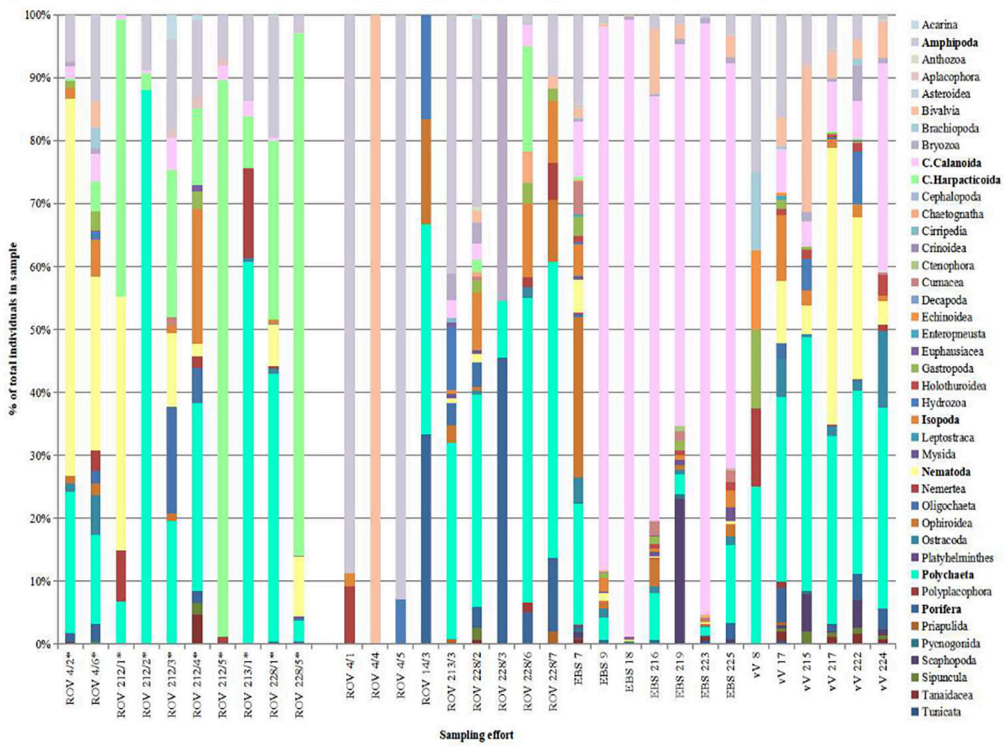

FIGURE 4 | Total percentage composition of taxonomic groups from biological samples taken in the Steinahóll region. *Denotes hydrothermally influenced sampling effort. Bold taxonomic names discussed in results/discussion.

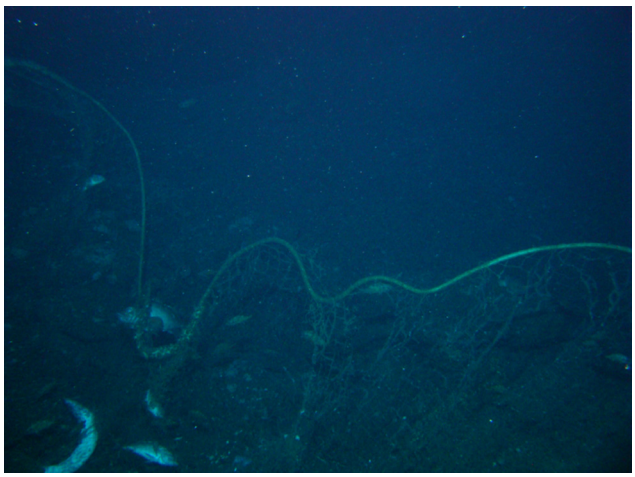

FIGURE 5 | Photo demonstrating fishing pressure example showing a discarded gill-net that has caught fresh fish, located near the Hafgufa hydrothermal vent field.

Carter, 1876, *Geodia* cf. *hentscheli* Cárdenas et al. (2010) and a species tentatively identified as *Cinachyrella* Wilson, 1925 sp. were highly present (**Supplementary Table 6**).

Hydrothermal fauna from Steinahóll vents

This section concentrates on the taxa where we have clear indications that they occur in the hydrothermal vent affected samples, namely the ROV deployments where bacterial mats or active venting were visible, as defined in **Table 1**, rather than those that can be considered usual Icelandic shelf fauna.

Copepoda, Harpacticoida. During the dive ROV 228, there were seven sampling stations, with almost all individuals coming from a net sample taken of bacterial mats (ROV 228/1) and a chimney top sampled with the sampling arm of the ROV (228/5). ROV 228/1 sampled 1,109 individuals, 6.4 times more than the next highest quantity, 173 individuals during ROV 212 (212/2 - Net: Vent field with chimneys). Both locations were under the direct influence of hydrothermal activity. A total of 27 morphospecies could be identified. The two species, *Tisbe* Lilljeborg, 1853 sp. nov. and *Amphiascus* Sars G.O., 1905 sp. nov., (**Figure 6**) occurred very abundantly at hydrothermally active sites and in less abundance at non-hydrothermal sites (228/1 – Net: Bacterial mats: total Harpacticoida = 334; *Tisbe* sp. nov. = 222, *Amphiascus* sp. nov. = 111; 228/5 – Arm: Chimney top: total Harpacticoida = 575; *Tisbe* sp. nov. = 568; **Figure 7**). These two samples were the only examples where we observed large quantities of Harpacticoida, with these two species almost encompassing the entirety of individuals sampled.

Out of 963 *Tisbe* specimens, only 24 were encountered at non-hydrothermal sites. Out of 153 *Amphiascus* specimens, only 1 was detected at a non-hydrothermal site. All non-hydrothermal sites with *Tisbe* and *Amphiascus* were located in the vicinity of vents and not in more distant samples taken by EBS and van Veen grab. Five additional copepod species (six *Ameira* Boeck, 1865 sp.1 specimens, one Tegastidae Sars G.O., 1904 sp.1 specimen, three additional singletons) were only detected at active venting sites. 20 copepod species were only encountered at non-hydrothermal sites, including 13 singletons and 3 doubletons.

Peracarida. At the Steinahóll region (vent and non-vent samples together), 3802 peracarids were sampled in total between 157 and 363 m depth. Of this 59.9% were Amphipoda, 19.2% Isopoda, 15.0% Cumacea, 3.6% Mysida, and 2.3% Tanaidacea. Peracarids occurred in all ROV samples except ROV 14. Most of the peracarids were provided by the EBS samples (2775 ind.), mainly from station EBS 7 (2341 individuals). Amphipods and isopods were determined on family level (**Supplementary Tables 1, 2**, respectively). Here, we observed a high taxonomic richness with at least 33 different amphipod families and 15 isopod families. The preliminary findings suggested that hydrothermal activity did not significantly affect the overall peracarid family composition.

Five hundred and nine amphipods were determined from the vent-influenced ROV-samples (**Supplementary Table 1**). 15.1% of these are Stenothoidae Boeck, 1871, with Amphilochidae Boeck, 1871 (3.9%) also represented in numbers that can be considered as non-stray specimens. Compared with ROV samples from areas not influenced by vents, there are more amphipods in general present, represented by fewer families. Families dominating the non-vent samples are Lysianassoidea Dana, 1849 (33%) Stenothoidae (15.2%) Pleustidae Buchholz, 1874 (14.7%), and Calliopiidae G.O. Sars, 1893 (6.9%) (**Figure 8**). Examples of Ampithoidae, Stenthoidae, and Calliopiidae can be seen in **Figure 9**.

The 15 isopod families sampled at Steinahóll have all been reported earlier from Icelandic waters (Brix et al., 2018b). In ROV samples with venting activity, isopods were collected only at two sampling sites (ROV212/2 – Net: Vent field with chimneys and ROV228/1 – Net: Bacterial mats). The families collected at hydrothermal vent sites, i.e., the Janiridae G.O. Sars, 1897 and the Gnathiidae Leach, 1814, were reported also outside the vent sites. Thus, no "stand out" Isopoda families were recorded from the vent-related samples.

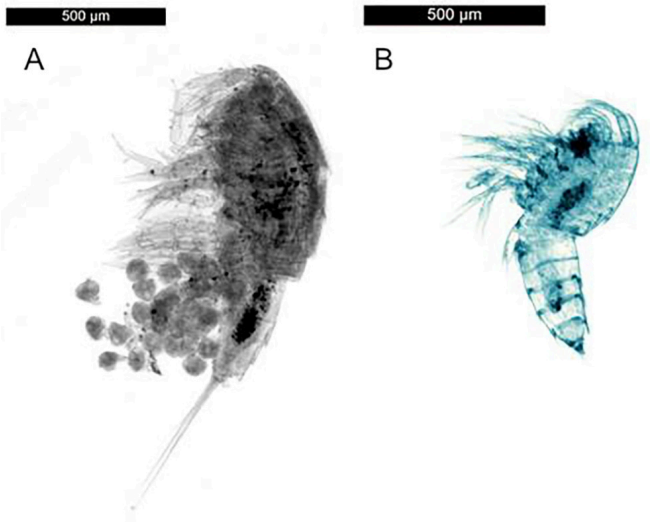

FIGURE 6 | Microscope images of **(A)** *Tisbe* sp. nov. (with nauplii), and **(B)** *Amphiascus* sp. nov.

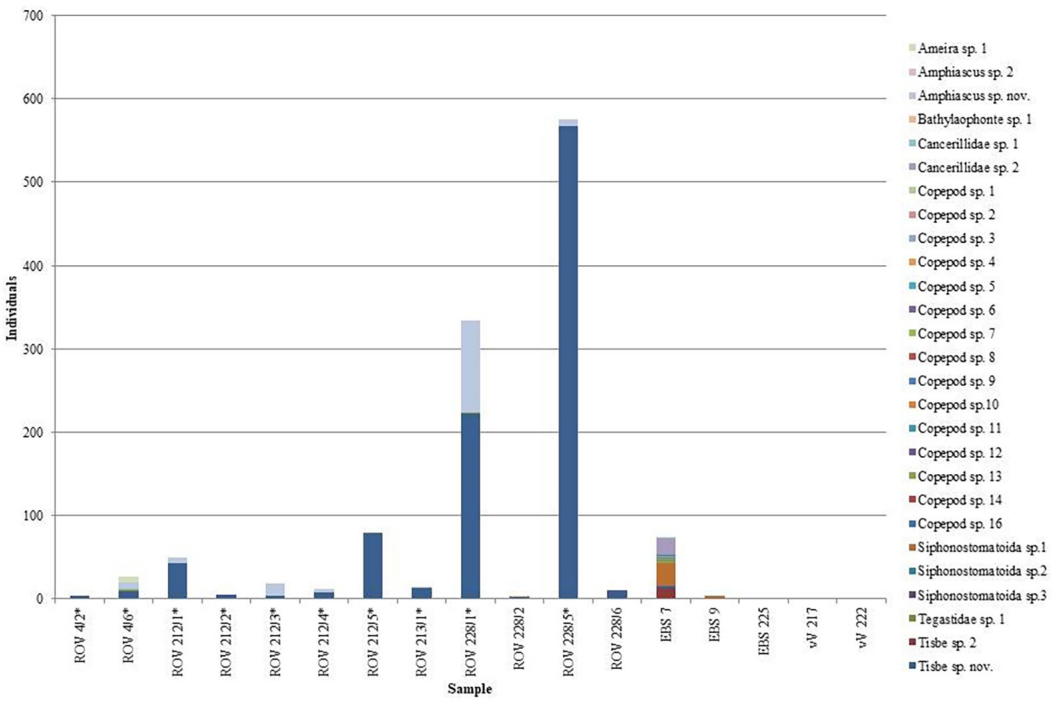

FIGURE 7 | Total individuals of Copepoda, Harpacticoida species taken during biological sampling during ROV, EBS, and vV deployments.

Polychaeta. A total of 4328 specimens of polychaetes representing 40 families were recorded in the samples from the Steinahóll area (**Supplementary Table 3**). About 60% of the specimens were collected by use of EBS, 25% by ROV and 15% by van Veen. The ROV samples taken from hydrothermal influenced sediments (9 samples) contained 1284 specimens representing 20 families of polychaetes, of which two, Dorvilleidae (530 specimens) and Capitellidae (466 specimens), accounted for more than 75% of the total number of specimens from these samples. Both families were also recorded from ROV, EBS and vV samples regarded as not hydrothermally influenced, but in far less quantities. Identification of specimens belonging to the two dominating families in hydrothermally influenced samples indicates that both families were represented by only a single species each, *Capitella* Blainville, 1828 sp. (Capitellidae) and *Mammiphitime* Orensanz, 1990 sp. (Dorvilleidae), both putative new to science (**Figure 10**).

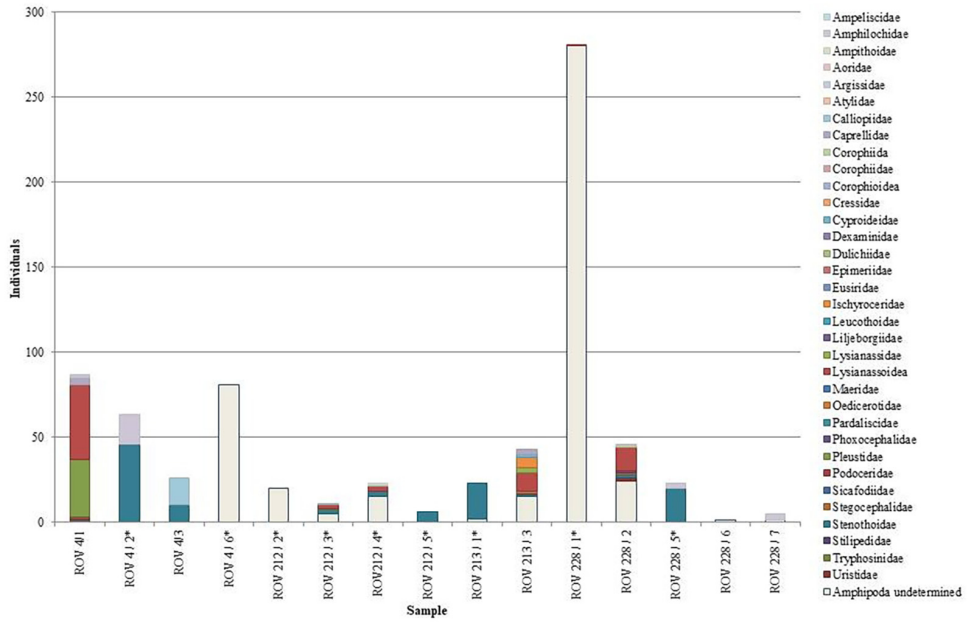

FIGURE 8 | Total individuals described to family level for Amphipoda during biological sampling of hydrothermally and non-hydrothermally influenced sites using ROV Phoca.

FIGURE 9 | Photographic plate demonstrating examples of the Amphipoda **(a)** Ampithoidae sp. (5 mm scale bar), **(b)** Stenothoidae sp. (1 mm scale bar), and **(c)** Calliopiidae sp. (5 mm scale bar) from ROV 212/4*.

Mollusca. A total of 1135 molluscs were present in sediment samples collected by ROV, EBS, and vV grab. Identification to morphospecies level yielded 27 bivalve species, 24 gastropod species, one polyplacophoran, and five scaphopod species. The majority of species were represented by a low number of specimens or by juveniles. No molluscs were recorded from vent-influenced ROV samples, except for two specimens recovered from bacterial mats at a diffuse flow site (ROV 228/1), representing one specimen each of the cimid *Cima inconspicua* Warén, 1993 and a juvenile buccinid *Colus* Röding, 1798 species.

Microbiology. The preliminary results of the microbial diversity show some accordance with other deep-sea hydrothermal vents (Dick, 2019), especially to the high-temperature vent field east of Grímsey, North of Iceland (Hannington et al., 2001; Marteinsson et al., 2013).

Cultivation results show high diversity of thermophilic, heterotrophic, and chemoautotrophic microorganisms belonging to bacterial and archaeal domains. These thermophilic taxa were cultivated from bacterial mats and chimney pieces stored anaerobically at 4°C before enrichments and isolation of strains performed at 65°C and above. Taxonomic identification was performed by sequencing the 16S rRNA genes from the isolates.

Preliminary results revealed bacterial strains belonging to different taxa such as *Thermotogales*, *Proteobacteria*, *Bacteroidetes,* and *Deinococcus*. Archaeal strains belonged mainly to the members of *Thermococcales, Archaeoglobales,* and *Thermoproteales* to some extent.

DISCUSSION

The presence of anhydrite chimneys, siliceous, and barite-bearing slabs from Steinahóll also resembles that of shallow-water vent sites further south along the Mid-Atlantic Ridge (MAR). Albeit

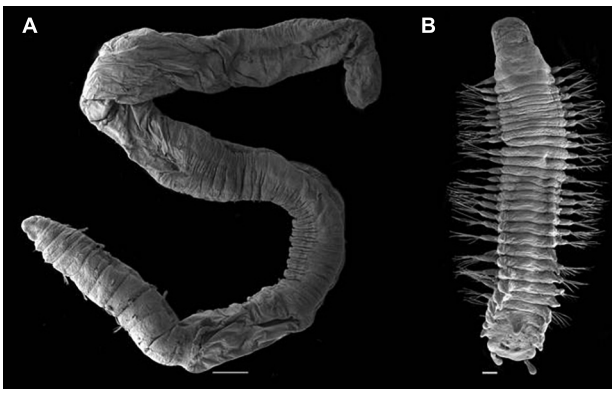

FIGURE 10 | Photographic plate demonstrating examples of the Polychaeta **(A)** *Capitella* sp. (500 μm scale bar) and **(B)** *Mammiphitime* sp. (100 μm scale bar).

at greater depth than Steinahóll, similar chimneys and slabs have been documented from the Menez Gwen and Bubbylon vent fields near 37°50′N in water depths between 800 and 1000 m (Colaço et al., 1998; Bogdanov et al., 2005; Marcon et al., 2013). Additionally, clear fluids have also been reported from the Grímsey vent field, north of Iceland (Hannington et al., 2001). Here, 250°C hot, boiling, and metal-depleted fluids are venting at a water depth of 400 m and form anhydrite chimneys, barite-rich slabs, and clay-rich mounds. The venting style at Steinahóll resembles both, Menez Gwen and Grímsey, with respect to venting of clear fluids and the presence of visible boiling.

Despite the (biological) limitation of working with higher taxon level at present state, the discovery of the vent sites is based on an exploratory expedition. Sampling, particularly with the ROV, was limited by the multidisciplinary character of each dive. The non-uniform sampling of the ROV in combination with the other gears led to limited options for community comparisons between the samples. ROV sampling focused on the lava pillows and ridge structures, whereas EBS and vV deployments had to be conducted in plain and/or soft-bottom areas. As expected, the use of different sampling gears was accompanied by distinctly different faunal elements. The deployment of the EBS and vV equipment in the detected vent sites was avoided to prevent any potential damage to the fragile structures.

Vent Fauna at Steinahóll Vent Sites

The present study describes a lower total number of taxonomic groups initially discovered in vent areas, compared with the fauna present in close proximity to the Steinahóll vent field, with *Lycopodina cupressiformis* (Porifera), *Capitella* sp. and *Mammiphitime* sp. (Polychaeta), *Tisbe* sp. nov., *Amphiascus* sp. nov. and a species of Stenothoidae (Crustacea) having a notable presence in vent-influenced samples. All apart from *L. cupressiformis* in this list await careful taxonomic checks as they may be new to science. Almost no sponges were found within the active venting and/or the surrounding area with diffuse seepage and bacterial growth, barring *L. cupressiformis*. This difference falls well within what has also been found on the Mohns Ridge further to the north, where also the cladorhizids *Asbestopluma furcata* and *L. cupressiformis* were among the very few thriving at hydrothermal vents, or in the very close enrichment zone surrounding the vents (Schander et al., 2010; Hestetun et al., 2017), potentially benefiting from the enhanced food availability (Hestetun et al., 2016).

The two stand-out polychaete species in the hydrothermally influenced samples, *Capitella* sp. and *Mammiphitime* sp., represent taxa well known from reduced shallow water environments (Oug, 1990; Blake et al., 2009). *Capitella* sp. was also recorded from the Kolbeinsey Ridge (Fricke et al., 1989), and may be the same species as our records of these taxa from Steinahóll. Polychaetes of the genus *Capitella* are considered to be opportunistic, typically occurring in high abundance in reduced environments (Blake et al., 2009; Silva et al., 2017) including shallow water hydrothermal vents (Gamenick et al., 1998; Sweetman et al., 2013). Specimens identified as *Mammiphitime* sp. from Steinahóll are morphologically similar to *Mammiphitime cosmetandra* (Oug, 1990) described from benthic algal-deposits at shallow water near Tromsø, northern Norway. However, the specimens differ in details related to morphology of the jaws as well as the number of segments, and is therefore regarded to constitute a separate, undescribed species.

The copepod species *Tisbe* sp. nov. and *Amphiascus* sp. nov., were extremely abundant in the bacterial mats at Steinahóll. The absence of these species in further distance to the ridge as well as the low abundance of these species at non-hydrothermal sites in the vicinity of vents, suggests that they have adapted to a life under extreme vent conditions. Since they are putative new species [only one formally described *Tisbe* species by Ivanenko et al. (2011), no description from *Amphiascus*], it is not possible yet to discuss distribution patterns and potential vent endemism of these species. *Tisbe* and *Amphiascus* are genera that often occur at deep-sea hydrothermal vents, in the direct vent vicinity (Gollner et al., 2010, 2016; Plum et al., 2017) as well as in the intertidal (Steinarsdóttir et al., 2003).

The amphipod-family Stenothoidae can be considered to be having at least one vent-associated species in the Steinahóll area. In the hydrothermally influenced samples, stenothoid amphipods were a dominant family, but they were also present out of the active areas. Similar opportunist behavior has been already pointed out for other stenothoids in the Lucky Strike vent fields, where the same species was collected at 1–2 m from the hydrothermal fluid emissions, among sponges, dead mussels, or gorgonians outside of the active hydrothermal areas (Bellan-Santini, 2005). Comparing that we observe only the family Stenothoidae as being vent influenced, with the observations of 20 families being vent-influenced along the entire Mid-Atlantic Ridge (Vinogradov, 1995; Bellan-Santini and Thurston, 1996; Desbruyères et al., 2001; Myers and Cunha, 2004; Bellan-Santini, 2005, 2006, 2007; Schander et al., 2010; Tandberg et al., 2012; Corbari and Sorbe, 2018), Steinahóll seems very limited in vent-influenced amphipods. However, most vent-influenced observations of amphipods tend to be one species to one vent, all seemingly endemic (e.g., Schander et al., 2010; Tandberg et al., 2012; Corbari and Sorbe, 2018 and references therein). Further identification to species level will show us if,

and how many, vent-adapted species are amongst the stenothoid Amphipoda of the Reykjanes Ridge. The composition of the isopod families collected in the Steinahóll area resembles the fauna collected at the Mohns Ridge (Schander et al., 2010), with members of the families Janiridae and Gnathiidae being present in the bacterial mats.

Non-vent Fauna at Steinahóll Vent Sites

The non-vent sponge fauna is a peculiar mix of typically boreal and temperate sponge species. The species *Geodia atlantica*, *G. barretti*, *G. macandrewii,* and *G. phlegraei* are all characteristic components of boreal tetractinellid sponge grounds (Klitgaard and Tendal, 2004; Cárdenas et al., 2013; Maldonado et al., 2017), while the hexactinellids *Pheronema carpenteri*, *Euplectella suberea*, *Hyalonema thomsoni*, *Aphrocallistes* cf. *beatrix, Asconema* spp., and Euretidae indet. are typical for more temperate grounds (e.g., Maldonado et al., 2017). In addition, there are also a number of temperate demosponges, e.g., *Geodia megastrella* and a tentative *Cinachyrella* species. The presence of *Geodia* cf. *hentscheli* is interesting as it is a very common component of arctic sponge grounds (normally found at negative temperatures) (Roberts et al., 2018; Meyer et al., 2019). However, Cárdenas and Rapp (2015) reported *G. hentscheli* and *G.* cf. *hentscheli* from further south on the Mid-Atlantic Ridge, and already then it was noted that the records were far outside the normal distribution and temperature range for the species. Most likely these southern records, as well as the numerous specimens observed in the Steinahóll area, represent a different and hereto undescribed species.

The molluscan fauna in Steinahóll is typical to that of southern Iceland (Madsen, 1949; Warén, 1989, 1991, 1993, 1996; Dijkstra et al., 2009) and western Norway (Bouchet and Warén, 1979, 1980, 1985, 1986, 1993; Warén, 1989, 1991, 1993, 1996; Høisæter, 2010). In fact, all live-collected species that have been determined to species level (34 species) are known to live in western Norway. Most species of this set have large distribution ranges, typically including the continental margins of western Europe.

The comparison of the Steinahóll molluscan fauna (57 live-collected species) with the one reported from the Mohns Ridge hydrothermal vent sites (28 reported species; Schander et al., 2010) highlights both differences and similarities. Typical vent fauna, such as the genera described by Warén and Bouchet (2001), have been found at neither the Mohns Ridge nor in Steinahóll; with both sites displaying a species set characteristic of lower shelf, upper bathyal species with large distribution areas. At species level, only the bivalves *Bathyarca frielei* (Friele, 1877) and *Lyonsiella abyssicola* Sars G.O., 1878 are present in both areas. The malacofauna of the Mohns Ridge are characteristic of those found on the continental margins off northern Iceland, Norway, and Russia.

Non-vent samples in this study observe similar peracarid crustacean family composition described of the background Icelandic fauna in Brix et al. (2018a,b). For peracarid crustaceans, the shelf may function as a pathway from Norway to Iceland and farther on to Greenland or vice versa. While for amphipods, the differences between north and south of the Greenland-Iceland-Faroe (GIF) Ridge can already be observed on family level, for isopods depth gradients are more important. There are typical shallow-water families and typical deep-sea families, with the exception being Munnopsidae. They are the only asellote isopods with clearly proven swimming abilities (Schnurr et al., 2014, 2018; Bober et al., 2018; Malyutina et al., 2018) crossing the MAR and the GIF Ridge.

Comparisons to Hydrothermal Vents in the North Atlantic and Arctic

Marine hydrothermally active sites in Icelandic waters have been reported from around 350 m water depth on the northern end of the Reykjanes Ridge (Olafsson et al., 1991), around 100 m water depth on the Kolbeinsey Ridge (Fricke et al., 1989), and at 20–60 m depth in the fjord Eyjafjörður (Marteinsson et al., 2001; Eythorsdottir et al., 2016). Similar to the Steinahóll vent field, no vent-endemic, chemosynthetic taxa have been reported from these shallow water vents (Fricke et al., 1989). Absence of vent-endemic species was also reported from the Arctic Jan Mayen vent fields at 550–720 m depth at the AMOR ridge (Schander et al., 2010).

In comparison, the macrofauna of the deeper MAR vent fields is characterized by the presence of a high abundance of vent-endemic and chemosynthetic taxa, such as the shrimps *Miricaris* and *Rimicaris*, the gastropod *Peltospira* (Warén and Bouchet, 2001), or the bivalve *Bathymodiolus* (e.g., Desbruyères et al., 2006; Wheeler et al., 2013). The Arctic Loki's Castle vent field on the Knipovich Ridge in 2350 m also supports an endemic fauna (Pedersen et al., 2010; Kongsrud and Rapp, 2012; Tandberg et al., 2012; Sweetman et al., 2013; Kongsrud et al., 2017). In general, these Arctic deep sea vents support a completely different fauna from the deep Atlantic vents south of Iceland (Bellan-Santini, 2005).

Shallow water vents are typically colonized by a subset of local background fauna (Dando, 2010). Species diversity commonly declines along a transect toward the vent due to increasing temperatures, sulfide concentration and decreasing pH (Dando, 2010). Whilst we were unable to test this, we observed the presence of only a few species occurring in high abundance in the vent-influenced samples. Further, the absence, or sporadic presence, of those taxa we found within vent-influenced samples in the surrounding areas, is also observed from other shallow water vents (Fricke et al., 1989; Dando, 2010; Sweetman et al., 2013).

Amphipoda as vent-associated fauna has been proven by *Exitomelita sigynae* from Loki's Castle north of Iceland (Tandberg et al., 2012) and *Dulichiopsis dianae* from the TAG hydrothermal vent field along the MAR (Corbari and Sorbe, 2018), with each species being restricted to a single vent site. The amphipod species found in the bacterial mats at Steinahóll belongs to different families than the species described from the North (Loki) and requires further taxonomic attention to confirm the theory of a vent-associated species new to science. The two reported vent-associated isopod families Janiridae G.O. Sars, 1897 and Gnathiidae Leach, 1814 were also reported as present by Schander et al. (2010) from the Mohns Ridge.

For harpacticoid copepods preliminary results based on COI data and morphological identification (Eva Paulus and Sabine

Gollner, unpublished data) show that the same harpacticoid *Tisbe* species can be found at Steinahóll as at the shallow water vent in the fjord Eyjafjörður. This connectivity could suggest more undiscovered shallow-water vents between the two sites and supports the hypothesis of the shelf as a pathway of fauna and linking the north and south of Iceland.

At present, the knowledge about organisms associated with hydrothermal vents and other reduced environments in Icelandic waters is essentially limited to the literature discussed here and the present study of Steinahóll. Additional sampling of vent communities in Icelandic waters is fundamental in order to understand biodiversity, species composition and distribution of species associated with these extreme habitats. Along the Reykjanes Ridge, potential hydrothermal activity was detected in deeper areas during the MSM75 expedition. Exploration of fauna from these potential deeper, hydrothermally active sites may provide new insight into bathymetric distributions of different vent and seep species, as well as uncover the potential presence of a specialized chemosynthetic fauna at greater depth, similar to what is described from deep-sea vents at the MAR and AMOR.

How Vulnerable Is Steinahóll?

Meeting many of the criteria when asking "what constitutes a VME?" such as uniqueness, functional significance, fragility, structural complexity, and certain life history traits, the Steinahóll vent sites should be protected accordingly. Despite a ban in the area of bottom and midwater trawling by the Icelandic government (Reg. No. 310/2007) the area is still under stress from fishing, with numerous observed occasions of abandoned long-line and gill-net fishing equipment. The picture of the faunal composition is presently limited to higher taxon level and family level, but the species determination for several taxa is in progress and will bring more light into the macrofauna associated with the vent sites, as well as other VMEs in the close vicinity.

CONCLUSION

Although Steinahóll is known as a geological active area since the 1990s, the published materials remain sparse. Through future cross-institute collaborations, more work is to be expected on species level based on the samples presented from IceAGE_RR (MSM75), as well as analysis of recent and previous photo/video material. As a first impression, we conclude that shallow vent sites north and south of Iceland are comparable. The vent sites themselves show little to no megafauna, but meio- and macrofauna taxa associated with reduced environments in North Atlantic are visible in the microscopic view, mainly harpacticoid copepods occurring with species new to science, and dorvelleid worms hiding in bacterial mats not visible on video material, only in physical samples. We do not observe the characteristic chemosynthetic fauna seen in deep-sea hydrothermal vents, but rather species belonging to genera typically associated with shallow-water reduced environments. The bacterial mats and chimneys house unique fauna not observed in the surrounding environment. As more results on species level will be expected in the future, we may conclude here that the microscopic view already reveals a vulnerable unique environment.

DATA AVAILABILITY STATEMENT

All datasets generated for this study are included in the article/**Supplementary Material**.

AUTHOR CONTRIBUTIONS

CD and SB organized the expedition MSM75. JT, CD, and SB contributed conception and design of the study. SB and JT organized the database. SB, IF, AHT, KL, and JT collected and processed the specimens on board. HR determined the Porifera presence and absence during ROV deployments based on video analysis. TK performed 3D reconstruction of vent. JT, SB, SP, and DP wrote the first draft of the manuscript. JT, SB, KL, A-NL, AHT, IF, SP, ML, LH, DP, SG, EP, JK, TK, and HR wrote sections of the manuscript. ML, SP, and JT created the figures. All the authors contributed to manuscript revision, read and approved the submitted version.

FUNDING

The biological part of cruise MSM75 and the follow-up sorting workshop was financed by the German Science Foundation under grant BR3843/5-1 (SB). The costs for the geological dives of ROV and AUV on the cruise were provided by GEOMAR/Helmholtz-Foundation (to CD). JT was completely supported by the German Science Foundation under contract no. BR 3843/5-1. HR and AT received funding from the European Union's Horizon 2020 research and innovation programme through the SponGES project (grant agreement No 679849). AT payed in part by Norwegian Species Initiative project 16_18-NorAmph2. This document reflects only the authors' view and the Executive Agency for Small and Medium-sized Enterprises (EASME) is not responsible for any use that may be made of the information it contains.

ACKNOWLEDGMENTS

We would like to dedicate this manuscript to the memory of HR, a dear friend and colleague who passed away during the review phase of this manuscript. We miss him and would like to use this paragraph here to thank him for his enthusiastic support of the IceAGE project and his highly valuable scientific contributions. We would like to thank the following people for their key contributions to our manuscript: the crew of *MS Merian* during IceAGE_RR (MSM75). Antje Fischer (TA DZMB HH), Karen Jeskulke (TA DZMB HH), Sarah Menke (TA DZMB WHV), and Franziska Iwan (TA WHV) for their support in logistics and organization of the sorting workshop at the University of Iceland's Research Centre in Sandgerði and all necessary database entries in the whole progress. Steinunn Hilma Ólafsdóttir for sample storage of all coral pieces and Icelandic fishing regulation consultation. Guðmundur Guðmundsson for

helping with sample storage at the Natural History Museum Iceland. The late Guðmundur V. Helgason for his efforts into sample sorting. Hanna María Kristjánsdóttir for her assistance in setting up the sorting workshop in Sandgerði. Jon Tomas Magnusson, Anna Huras, and Carolin Uhlir for their assistance in sorting physical specimens and finally Thorge von Bosse and the ROV team from GEOMAR for their contributions in helping us obtain high quality video and image material.

SUPPLEMENTARY MATERIAL

The Supplementary Material for this article can be found online at: https://www.frontiersin.org/articles/10.3389/fmars.2021.520713/full#supplementary-material

Supplementary Figure 1 | Interactive 3D model of the Steinahóll largest venting field, Hafgufa.

Supplementary Table 1 | Amphipoda family composition at Steinahóll vent fields. *: Hydrothermally influenced sample.

Supplementary Table 2 | Isopoda family composition at Steinahóll vent fields. *: Hydrothermally influenced sample.

Supplementary Table 3 | Polychaeta family composition at Steinahóll vent fields. *: Hydrothermally influenced sample.

Supplementary Table 4 | Mollusca family composition at Steinahóll vent fields. *: Hydrothermally influenced sample.

Supplementary Table 5 | Copepoda Harpacticoida family composition at Steinahóll vent fields. *: Hydrothermally influenced sample.

Supplementary Table 6 | Porifera presence/absence during ROV deployments based on video analysis at Steinahóll vent fields.

REFERENCES

Bani-Hassan, N., Iyer, K., Rüpke, L. H., and Borgia, A. (2012). Controls of bathymetric relief on hydrothermal fluid flow at mid-ocean ridges. *Geochem. Geophys. Geosystems* 13:Q05002. doi: 10.1029/2012GC004041

Bellan-Santini, D. (2005). Stenothoidae (Crustacea, Amphipoda) of hydrothermal vents and surroundings on the mid-atlantic ridge, azores triple junction zone. *J. Nat. History* 39, 3435–3452. doi: 10.1080/00222930500345749

Bellan-Santini, D. (2006). Rhachotropis species (Crustacea: Amphipoda: Eusiridae) of hydrothermal vents and surroundings on the Mid-Atlantic Ridge, Azores Triple Junction Jone. *J. Nat. History* 40, 1407–1424.

Bellan-Santini, D. (2007). New amphipods from hydrothermal vent environments on the mid-atlantic ridge, azores triple junction zone. *J. Nat. History* 41, 567–596. doi: 10.1080/00222930701262537

Bellan-Santini, D., and Thurston, M. (1996). Amphipoda of the hydrothermal vents along the mid-Atlantic Ridge. *J. Nat. History* 30, 685–702. doi: 10.1080/00222939600770381

Bianchi, G. G., Hall, I. R., McCave, I. N., and Joseph, L. (1999). Measurement of the sortable silt current speed proxy using the sedigraph 5100 and coulter multisizer IIe: precision and accuracy. *Sedimentology* 46, 1001–1014. doi: 10.1046/j.1365-3091.1999.00256.x

Blake, J. A., Grassle, J. P., and Eckelbarger, K. J. (2009). Capitella teleta, a new species designation for the opportunistic and experimental *Capitella sp*. I, with a review of the literature for confirmed records. *Zoosymposia* 2, 25–53. doi: 10.11646/zoosymposia.2.1.6

Bober, S., Brix, S., Riehl, T., Schwentner, M., and Brandt, A. (2018). Does the midatlantic ridge affect the distribution of benthic crustaceans across the atlantic ocean? *Deep-Sea Res. Part II.* 148, 91–104. doi: 10.1016/j.dsr2.2018.02.007

Bogdanov, Y. A., Lein, A. Y., and Sagalevich, A. M. (2005). Chemical composition of the hydrothermal deposits of the Menez Gwen vent field (Mid-Atlantic Ridge). *Oceanology* 45, 849–856.

Bouchet, P., and Warén, A. (1979). The abyssal molluscan fauna of the Norwegian Sea and its relation to other faunas. *Sarsia* 64, 211–243. doi: 10.1080/00364827.1979.10411383

Bouchet, P., and Warén, A. (1980). Revision of the northeast Atlantic bathyal and abyssal turridae (Mollusca, Gastropoda). Milano, Italy. *J. Molluscan Stud.* 8, 1–119. doi: 10.1093/mollus/46.Supplement_8.1

Bouchet, P., and Warén, A. (1985). Revision of the northeast Atlantic bathyal and abyssal neogastropoda excluding turridae (Mollusca, Gastropoda). *J. Molluscan Stud.* 8, 124–296. doi: 10.5962/bhl.title.140763

Bouchet, P., and Warén, A. (1986). Revision of the northeast atlantic bathyal and abyssal aclididae, eulimidae, epitoniidae. *Bollettino Malacol. Suppl.* 2, 297–576. doi: 10.5962/bhl.title.140762

Bouchet, P., and Warén, A. (1993). Revision of the northeast Atlantic bathyal and abyssal *Mesogastropoda*. *Bollettino Malacologico. Suppl.* 3, 577–840. doi: 10.5962/bhl.title.140732

Brenke, N. (2005). An epibenthic sledge for operations on marine soft bottom and bedrock. *Mar. Technol. Soc. J.* 39, 10–21. doi: 10.4031/002533205787444015

Brix, S., Lörz, A.-N., Jażdżewska, A. M., Hughes, L., Tandberg, A. H. S., Pabis, K., et al. (2018a). Amphipod family distributions around Iceland. *ZooKeys* 731, 1–53. doi: 10.3897/zookeys.731.19854

Brix, S., Stransky, B., Malyutina, M., Pabis, K., Svavarsson, J., and Riehl, T. (2018b). Distributional patterns of isopods (Crustacea) in Icelandic and adjacent waters. *Mar. Biodiversity* 48, 783–811. doi: 10.1007/s12526-018-0871-z

Brix, S., Meißner, K., Stransky, B., Halanych, K. M., Jennings, R. M., Kocot, K. M., et al. (2014a). The IceAGE project – a follow up of BIOICE. *Polish Polar Res.* 35, 141–150. doi: 10.2478/popore-2014-0010

Brix, S., Svavarsson, J., and Leese, F. (2014b). A multi-gene analysis reveals multiple highly divergent lineages of the isopod Chelator insignis (Hansen, 1916) south of Iceland. *Polish Polar Res.* 35, 225–242. doi: 10.2478/popore-2014-0015

Brix, S., and Svavarsson, J. (2010). Distribution and diversity of desmosomatid and nannoniscid isopods (Asellota) on the Greenland-Iceland-Faeroe Ridge. *Polar Biol.* 33, 515–530.

Brix, S., and Devey, C. W. (2019). Stationlist of the IceAGE project (Icelandic marine Animals: Genetics and Ecology) expeditions. *Mar. Data Arch.* doi: 10.14284/349

Cárdenas, P., and Rapp, H. T. (2015). Demosponges from the northern mid-atlantic ridge shed more light on the diversity and biogeography of North Atlantic deep-sea sponges. *J. Mar. Biol. Assoc. UK* 95, 1475–1517. doi: 10.1017/S0025315415000983

Cárdenas, P., Rapp, H. T., Klitgaard, A. B., Best, M., Thollesson, M., and Tendal, O. S. (2013). Taxonomy, biogeography and DNA barcodes for Geodia species (Porifera, Demospongiae, Astrophorida) in the Atlantic Boreo-Arctic region. *Zool. J. Linnean Soc.* 169, 251–311. doi: 10.1111/zoj.12056

Cárdenas, P., Rapp, H. T., Schander, C., and Tendal, O. S. (2010). Molecular taxonomy and phylogeny of the Geodiidae (Porifera, Demospongiae, Astrophorida) – combining phylogenetic and Linnaean classification. *Zool. Scripta* 39, 89–106. doi: 10.1111/j.1463-6409.2009.00402.x

Colaço, A., Desbruyères, D., Comtet, T., and Alayse, A.-M. (1998). Ecology of the menez gwen hydrothermal vent field (Mid-Atlantic Ridge/Azores Triple Junction). *Cahiers Biol. Mar.* 39, 237–240.

Copley, J. T. P., Tyler, P. A., Sheader, M., Murton, B. J., and German, C. R. (1996). Megafauna from sublittoral to abyssal depth along the Mid-Atlantic Ridge south of Iceland. *Oceanol. Acta* 19, 549–559.

Corbari, L., and Sorbe, J. C. (2018). First observation of the behaviour of the deep-sea amphipod *Dulichiopsis dianae* sp. nov. (Senticaudata, Dulichiidae) in the TAG hydrothermal vent field) Mid-Atlantic Ridge). *Mar. Biodiversity* 48, 631–645. doi: 10.1007/s12526-017-0788-y

Dando, P. R. (2010). "Biological communities at marine shallow-water vent and seep sites," in *The Vent and Seep Biota. Topics in Geobiology*, ed. S. Kiel (Dordrecht: Springer), doi: 10.1007/978-90-481-9572-5_11

Dauvin, J.-C., Alizier, S., Weppe, A., and Gudmundsson, G. (2012). Diversity and zoogeography of Icelandic deep-sea Ampeliscidae (Crustacea: Amphipoda).

Deep-Sea Res. Part I: Oceanographic Res. Papers 68, 12–23. doi: 10.1016/j.dsr.2012.04.013

DeMets, C., Gordon, R. G., Argus, D. F., and Stein, S. (1990). Current plate motions. *Geophys. J. Int.* 101, 425–478. doi: 10.1111/j.1365-246X.1990.tb06579.x

Desbruyères, D., Almeida, A., Biscoito, A., Comtet, T., Khripounoff, A., LeBris, N., et al. (2000). A review of the distribution of hydrothermal vent communities along the northern Mid-Atlantic Ridge: dispersal vs. environmental controls. *Hydrobiologia* 440, 201–216.

Desbruyères, D., Biscoito, T., Caprais, J. C., Colaço, A., Comtet, T., Crassous, P., et al. (2001). Variations in deep-sea hydrothermal vent communities on the Mid-Atlantic Ridge near the Azores plateau. *Deep-Sea Res. Part I* 48, 1325–1346. doi: 10.1016/S0967-0637(00)00083-2

Desbruyères, D., Segonzac, M., and Bright, M. (2006). *Handbook of Deep-Sea Hydrothermal Vent Fauna*, 2ed Edn. Linz: Biologiezentrum der Oberosterreichische Landesmuseen.

Dick, G. J. (2019). The microbiomes of deep-sea hydrothermal vents: distributed globally, shaped locally. *Nat. Rev. Microbiol.* 17, 271–283. doi: 10.1038/s41579-019-0160-2

Dijkstra, H. H., Warén, A., and Guðmunsson, G. (2009). Pectinoidea (Mollusca: Bivalvia) from Iceland. *Mar. Biol. Res.* 5, 207–243. doi: 10.1080/17451000802425643

Eythorsdottir, A., Omarsdottir, S., and Einarsson, H. (2016). Antimicrobial activity of marine bacterial symbionts retrieved from shallow water hydrothermal vents. *Mar. Biotechnol.* 18, 293–300. doi: 10.1007/s10126-016-9695-7

Foulger, G. R., and Anderson, D. L. (2005). A cool model for the Iceland hotspot. *J. Volcanol. Geothermal Res.* 141, 1–22. doi: 10.1016/j.jvolgeores.2004.10.007

Fricke, H., Giere, O., Stetter, K., Alfredsson, G. A., Kristjansson, J. K., Stoffers, P., et al. (1989). Hydrothermal vent communities at the shallow subpolar Mid-Atlantic Ridge. *Mar. Biol.* 102, 425–429. doi: 10.1007/BF00428495

Gamenick, I., Abbiati, M., and Giere, O. (1998). Field distribution and sulphide tolerance of Capitella capitata (Annelida: Polychaeta) around shallow water hydrothermal vents off Milos (Aegean Sea). a new sibling species? *Mar. Biol.* 130, 447–453. doi: 10.1007/s002270050265

German, C. R., Briem, J., Chin, C., Danielsen, M., Holland, S., James, R., et al. (1994). Hydrothermal activity on the Reykjanes ridge: the steinahóll vent-field at 63°06'N. *Earth Plan. Sci. Lett.* 121, 647–654. doi: 10.1016/0012-821X(94)90098-1

Gollner, S., Riemer, B., Martinez Arbizu, P., Le Bris, N., and Bright, M. (2010). Diversity of meiofauna from the 9u50'N East Pacific Rise across a gradient of hydrothermal fluid emissions. *PLoS One* 5:e12321. doi: 10.1371/journal.pone.0012321

Gollner, S., Stuckas, H., Kihara, T. C., Laurent, S., Kodami, S., and Martinez Arbizu, P. (2016). Mitochondrial DNA analyses indicate high diversity, expansive population growth and high genetic connectivity of vent copepods (Dirivultidae) across different Oceans. *PLoS One* 11:e0163776. doi: 10.1371/journal.pone.0163776

Hannington, M., Herzig, P., Stoffers, P., Scholten, J., Botz, R., Jonasson, I. R., et al. (2001). First observations of high-temperature submarine hydrothermal vents and massive anhydrite deposits off the north coast of Iceland. *Mar. Geol.* 177, 199–220. doi: 10.1016/S0025-3227(01)00172-4

Hestetun, J. T., Jørgensen, S. L., Dahle, H., Olsen, B. R., and Rapp, H. T. (2016). The microbiome and occurrence of methanotrophy in carnivorous sponges. *Front. Microbiol.* 7:1781. doi: 10.3389/fmicb.2016.01781

Hestetun, J. T., Tompkins-MacDonald, G., and Rapp, H. T. (2017). A review of carnivorous sponges from the boreal North Atlantic and Arctic Oceans. *Zool. J. Linnean Soc.* 181, 1–69. doi: 10.1093/zoolinnean/zlw022

Høisæter, T. (2010). The shell-bearing, benthic gastropods on the southern part of the continental slope off Norway. *J. Molluscan Stud.* 76, 234–244. doi: 10.1093/mollus/eyq003

Höskuldsson, Á, Hey, R., Kjartansson, E., and Guðmundsson, G. B. (2007). The reykjanes ridge between 63°10'N and Iceland. *J. Geodynam.* 43, 73–86. doi: 10.1016/j.jog.2006.09.003

Humphris, S. E., Herzig, P. M., Miller, D. J., Alt, J. C., Becker, K., Brown, D., et al. (1995). The Internal structure of an active sea-floor massive sulphide deposit. *Nature* 377, 713–716. doi: 10.1038/377713a0

Ivanenko, V. N., Ferrari, F. D., Defaye, D., Sarradin, P.-M., and Sarrazin, J. (2011). Description, distribution and microhabitats of a new species of Tisbe (Copepoda: Harpacticoida: Tisbidae) from a deep-sea hydrothermal vent field at the Mid-Atlantic Ridge (37°N, Lucky Strike). *Cahiers de Biol. Mar.* 52, 89–106.

Jakobsson, S. P., Jonsson, J., and Shido, F. (1978). Petrology of the Western Reykjanes Peninsula, Iceland. *J. Petrol.* 19, 669–705. doi: 10.1093/petrology/19.4.669

Jochumsen, K., Schnurr, S. M., and Quadfasel, D. (2016). Bottom temperature and salinity distribution and its variability around Iceland. *Deep-Sea Res. Part I: Oceanographic Res. Papers* 111, 79–90. doi: 10.1016/j.dsr.2016.02.009

Johnsson, G. L., and Jakobsson, S. P. (1985). Structure and peterology of the Reykjanes Ridge between 62°55'N and 63°48'N. *J. Geophys. Res.* 90, 10073–10083. doi: 10.1029/JB090iB12p10073

Keeton, J. A., Searle, R. C., Parsons, B., White, R. S., Murton, B. J., Parson, L. M., et al. (1997). Bathymetry of the Reykjanes Ridge. *Mar. Geophys. Res.* 19, 55–64. doi: 10.1023/A:1004266721393

Klitgaard, A. B., and Tendal, O. S. (2004). Distribution and species composition of mass occurrences of large-sized sponges in the northeast Atlantic. *Prog. Oceanography* 61, 57–98. doi: 10.1016/j.pocean.2004.06.002

Kongsrud, J. A., Eilertsen, M. H., Alvestad, T., Kongshavn, K., and Rapp, H. T. (2017). New species of Ampharetidae (Annelida: Polychaeta) from the Arctic Loki Castle vent field. *Deep Sea Res. Part II: Top. Stud. Oceanography* 137, 232–245. doi: 10.1016/j.dsr2.2016.08.015

Kongsrud, J. A., and Rapp, H. T. (2012). Nicomache (Loxochona) lokii sp. nov. (Annelida: Polychaeta: Maldanidae) from the Loki's Castle vent field—an important structure builder in an Arctic vent system. *Pol. Biol.* 35, 161–170.

Kwasnitschka, T., Koeser, K., Sticklus, J., Rothenbeck, M., Weiss, T., Wenzlaff, E., et al. (2016). DeepSurveyCam – a deep ocean optical mapping system. *Sensors* 16:164. doi: 10.3390/s16020164

LeBris, N., Arnaud-Haond, S., Beaulieu, S., Cordes, E., Hilario, A., Rogers, A., et al. (2016). "Hydrothermal vents and cold seeps," in *World Ocean Assess*, eds S. van de Gaever, and H. Watanabe (Cambridge: Cambridge University Press), 1–18.

Madsen, F. J. (1949). Marine bivalvia". *Zool. Iceland* 4, 1–166.

Maldonado, M., Aguilar, R., Bannister, R. J., Bell, J., Conway, K. W., Dayton, P. K., et al. (2017). "Sponge grounds as key marine habitats: a synthetic review of types, structure, functional roles and conservation concerns," in *Marine Animal Forests – The Ecology of Benthic Biodiversity Hotspots*, eds S. Rossi, L. Bramanti, A. Gori, and C. Orejas (Berlin: MeteorSpringer).

Malyutina, M., Frutos, I., and Brandt, A. (2018). Diversity and distribution of the deep-sea Atlantic *Acanthocope* (Crustacea, Isopoda, Munnopsidae), with description of two new species. *Deep-Sea Res. I.* 148, 130–150. doi: 10.1016/j.dsr2.2017.11.003

Marcon, Y., Sahling, H., Borowski, C., Santos Ferreira, dos, C., Thal, J., et al. (2013). Megafaunal distribution and assessment of total methane and sulfide consumption by mussel beds at Menez Gwen hydrothermal vent, based on geo-referenced photomosaics. *Deep-Sea Res. I.* 75, 93–109. doi: 10.1016/j.dsr.2013.01.008

Marteinsson, V. T., Kristjánsson, J. K., Kristmannsdóttir, H., Sæmundsson, K., Hannignton, M., Petursdottir, S. K., et al. (2001). Discovery and description of giant submarine smectite cones on the seafloor in eyjafjordur, northern iceland, and a novel thermal microbial habitat. *Appl. Eviron. Microbiol.* 67, 827–833. doi: 10.1128/AEM.67.2.827-833.2001

Marteinsson, V. T., Rúnarsson, Á, Stefánsson, A., Thorsteinsson, T., Jóhannesson, T., Magnússon, S. H., et al. (2013). Microbial communities in the subglacial waters of the Vatnajökull ice cap, Iceland. *ISME J.* 7, 427–437. doi: 10.1038/ismej.2012.97

Martin, E., Paquette, J. L., Bosse, V., Ruffet, G., Tiepolo, M., Sigmarsson, O., et al. (2011). Geodynamics of rift-plume interaction in Iceland as constrained by new 40Ar/39Ar and in situ U-Pb zircon ages. *Earth Planetary Sci. Lett.* 311, 28–38. doi: 10.1016/j.epsl.2011.08.036

Meißner, K., Fiorentino, D., Schnurr, S., Martinez Arbizu, P., Huettmann, F., Holst, S., et al. (2014). Distribution of benthic marine invertebrates at northern latitudes — an evaluation applying multi-algorithm species distribution models. *J. Sea Res.* 85, 241–254. doi: 10.1016/j.seares.2013.05.007

Meyer, H. K., Roberts, E. M., Rapp, H. T., and Davies, A. J. (2019). Spatial patterns of arctic sponge ground fauna and demersal fish are detectable in autonomous underwater vehicle (AUV) imagery. *Deep-Sea Res. I* 153:103137. doi: 10.1016/j.dsr.2019.103137

Murton, B. J., and Parson, L. M. (1993). Segmentation, volcanism and deformation of oblique spreading centres: a quantitative study of the

Reykjanes Ridge. *Tecto* 222, 237–257. doi: 10.1016/0040-1951(93)90051-K

Myers, A. A., and Cunha, M. R. (2004). New and little known corophiidean amphipods from the Lucky Strike hydrothermal vent, Mid-Atlantic Ridge. *J. Mar. Biol. Assoc. UK* 84, 1019–1025. doi: 10.1017/S0025315404010343h

Olafsson, J., Thors, K., and Cann, J. R. (1991). A sudden cruise off Iceland. *RIDGE Events* 2, 35–38.

OSPAR (2008). *). Agreement 2008–07. Description of habitats on the OSPAR list of threatened and/or declining species and habitats, 2008*. Available online at: https://www.ospar.org/convention/agreements/ (Accessed 10 September, 2017)

OSPAR (2014). *OSPAR Recommendation 2014/11 on Furthering the Protection and Conservation of Hydrothermal Vents/fields Occurring on Oceanic Ridge in Region V of the OSPAR Maritime Area, Annex 16, 2014*. Available online at: https://www.ospar.org/convention/agreements/, https://www.ospar.org/meetings/archive?Q=&a=&y=1993&s= (accessed 10 September, 2017)

Oug, E. (1990). Morphology, reproduction, and development of a new species of Ophryotrocha (Polychaeta: Dorvilleidae) with strong sexual dimorphism. *Sarsia* 75, 19–201. doi: 10.1080/00364827.1990.10413447

Pałgan, D., Devey, C. W., and Yeo, I. A. (2017). Volcanism and hydrothermalism on a hotspot–influenced ridge: comparing Reykjanes Peninsula and Reykjanes Ridge. Iceland. *J. Volcanol. Geothermal Res.* 348, 62–81. doi: 10.1016/j.jvolgeores.2017.10.017

Palmer, M., Kasper, K., van Benthem, K. J., Arni, M., Berg, C. W., Anders, N., et al. (1995). Dissolved methane and hydrogen in the Steinahóll hydrothermal plume, 63°N, Reykjanes Ridge. *Geol. Soc. London Special Publications* 87, 111–120. doi: 10.1144/GSL.SP.1995.087.01.10

Pedersen, G. B. M., and Grosse, P. (2014). Morphometry of subaerial shield volcanoes and glaciovolcanoes from Reykjanes Peninsula, Iceland: effects of eruption environment. *J. Volcanol. Geothermal Res.* 282, 115–133. doi: 10.1016/j.jvolgeores.2014.06.008

Pedersen, R. B., Rapp, H. T., Thorseth, I. H., Lilley, M. D., Barriga, F. J. A. S., Baumberger, T., et al. (2010). Discovery of a black smoker vent field and vent fauna at the Arctic Mid-Ocean Ridge. *Nat. Commun.* 1:126. doi: 10.1038/ncomms1124

Petersen, S., Kuhn, K., Kuhn, T., Augustin, N., Hékinian, R., Franz, L., et al. (2009). The geological setting of the ultramafic-hosted Logatchev hydrothermal field (14°45'N, Mid-Atlantic Ridge) and its influence on massive sulfide formation. *Lithos* 112, 40–56. doi: 10.1016/j.lithos.2009.02.008

Plum, C., Pradillon, F., Fujiwara, Y., and Sarrazin, J. (2017). Copepod colonization of organic and inorganic substrata at a deep-sea hydrothermal vent site on the Mid-Atlantic Ridge. *Deep Sea Res. II* 137, 335–348. doi: 10.1016/j.drs2.2016.06.008

Riehl, T., Brenke, N., Brix, S., Driskell, A., Kaiser, S., and Brandt, A. (2014). Field and laboratory methods for DNA studies on deep-sea isopod crustaceans. *Polish Pol. Res.* 35, 203–224. doi: 10.2478/popore-2014-0018

Roberts, E. M., Mienis, F., Rapp, H. T., Hanz, U., Meyer, H. K., and Davies, A. J. (2018). Oceanographic setting and short-timescale environmental variability at an Arctic seamount sponge ground. *Deep-Sea Res. I.* 138, 98–113. doi: 10.1016/j.dsr.2018.06.007

Sandwell, D. T., Müller, R. D., Smith, W. H. F., Garcia, E., and Francis, R. (2014). New global marine gravity model from CryoSat-2 and Jason-1 reveals buried tectonic structure. *Science* 346, 65–67. doi: 10.1126/science.1258213

Schander, C., Rapp, H. T., Kongsrud, J. A., Bakken, T., Berge, J., Cochrane, S., et al. (2010). The fauna of hydrothermal vents on the Mohn Ridge (North Atlantic). *Mar. Biol. Res.* 6, 155–171. doi: 10.1080/17451000903147450

Schnurr, S., Brandt, A., Brix, S., Fiorentino, D., Malyutina, M., and Svavarsson, J. (2014). Composition and distribution of selected munnopsid genera (Crustacea, Isopoda, Asellota) in Icelandic waters. *Deep-Sea Res. Part II* 84, 142–155. doi: 10.1016/j.dsr.2013.11.004

Schnurr, S., Osborn, K. J., Malyutina, M., Jennings, R. M., Brix, S., Svavarsson, J., et al. (2018). Hidden diversity in two species complexes of munnopsid isopods (Crustacea) at the transition between the northernmost North Atlantic and the Nordic Seas. *Mar. Biodiversity* 48, 813–843. doi: 10.1007/s12526-018-0877-6

Searle, R. C., Keeton, J. A., Owens, R. B., White, R. S., Mecklenburgh, R., and Parsons, B. (1998). The Reykjanes Ridge: structure and tectonics of a hot-spot-influenced, slow-spreading ridge, from multibeam bathymetry, gravity and magnetic investigations. *Earth Plan. Sci. Lett.* 160, 463–478. doi: 10.1016/S0012-821X(98)00104-6

Silva, C. F., Seixas, V. C., Barroso, R., Di Domenico, M., Amaral, A. C. Z., and Paiva, P. C. (2017). Demystifying the Capitella capitata complex (Annelida, Capitellidae) diversity by morphological and molecular data along the Brazilian coast. *PLoS One* 12:e0177760. doi: 10.1371/journal.pone.0177760

Steinarsdóttir, M. B., Ingólfsson, A., and Ólafsson, E. (2003). Seasonality of harpacticoids (Crustacea, Copepoda) in a tidal pool in subarctic south-western Iceland. *Hydrobiologia* 503, 211–221. doi: 10.1007/978-94-017-2276-6_22

Sweetman, A. K., Levin, L. A., Rapp, H. T., and Schander, C. (2013). Faunal trophic structure at hydrothermal vents on the southern Mohn's Ridge, Arctic Ocean. *Mar. Ecol. Prog. Ser.* 473, 115–131. doi: 10.3354/meps10050

Sæmundsson, K. (1979). Outline of the geology of Iceland. *Jökull* 29, 7–28.

Talwani, M., Windisch, C. C., and Langseth, M. G. (1971). Reykjanes Ridge crest: a detailed geophysical study. *J. Geophys. Res.* 76, 473–577. doi: 10.1029/JB076i002p00473

Tandberg, A. H. S., Rapp, H. T., Schander, C., Vader, W., Sweetman, A. K., and Berge, J. (2012). Exitomelita sigynae gen. et sp. nov.: a new amphipod from the Arctic Loki Castle vent field with potential gill ectosymbionts. *Pol. Biol.* 35, 705–716. doi: 10.1007/s.00300-011-1115-x

Tarasov, V. G., Gebruk, A. V., Mironov, A. N., and Moskalev, L. I. (2005). Deep-sea and shallow-water hydrothermal vent communities: two different phenomena? *Chem. Geol.* 224, 5–39. doi: 10.1016/j.chemgeo.2005.07.021

Thorarinsson, S. (1969). The lakagigar eruption of 1783. *Bull. Volcanol.* 33, 910–929. doi: 10.1007/BF02596756

Van Dover, C. L., Arnaud-Haond, S., Gianni, M., Helmreich, S., Huber, J. A., Jaeckel, A. L., et al. (2018). Scientific rationale and international obligations for protection of active hydrothermal vent ecosystems from deep-sea mining. *Mar. Policy* 90, 20–28. doi: 10.1016/j.marpol.2018.01.020

van Veen, J. (1933). Onderzoek naar het zandtransport von rivieren. *De Ingenieur* 48, 151–159.

Vinogradov, G. M. (1995). Amphipods from hydrothermal vents and cold seepings on the ocean bottom. *Oceanol. Russ. Acad. Sci.* 35, 69–74.

Warén, A. (1989). New and little known Mollusca from Iceland. *Sarsia* 74, 1–28. doi: 10.1080/00364827.1989.10413419

Warén, A. (1991). New and little known mollusca from Iceland and Scandinavia. *Sarsia* 76, 53–124. doi: 10.1080/00364827.1991.10413466

Warén, A. (1993). New and little known mollusca from Iceland and Scandinavia. Part 2. *Sarsia* 78, 159–201. doi: 10.1080/00364827.1993.10413534

Warén, A. (1996). New and little known mollusca from Iceland and Scandinavia. Part 3. *Sarsia* 81, 197–245. doi: 10.1080/00364827.1996.10413622

Warén, A., and Bouchet, P. (2001). Gastropoda and Monoplacophora from hydrothermal vents and seeps; new taxa and records. *Veliger* 44, 116–231.

Wheeler, A. J., Murton, B., Copley, J., Lim, A., Carlsson, J., Collins, P., et al. (2013). Moytirra: discovery of the first known deep-sea hydrothermal vent field on the slow-spreading Mid-Atlantic Ridge north of the Azores. *Geochem. Geophys. Geosystems* 14, 4170–4184. doi: 10.1002/ggge.20243

Conflict of Interest: PV and VM are employed by Matis Ltd.

The remaining authors declare that the research was conducted in the absence of any commercial or financial relationships that could be construed as a potential conflict of interest.

Publisher's Note: All claims expressed in this article are solely those of the authors and do not necessarily represent those of their affiliated organizations, or those of the publisher, the editors and the reviewers. Any product that may be evaluated in this article, or claim that may be made by its manufacturer, is not guaranteed or endorsed by the publisher.